Reexamination of the mandibular and dental morphology of the Early Jurassic mammaliaform *Hadrocodium wui*

ZHE-XI LUO, BHART-ANJAN S. BHULLAR, ALFRED W. CROMPTON, APRIL I. NEANDER, and TIMOTHY B. ROWE

Luo, Z.-X., Bhullar, B.-A.S., Crompton, A.W., Neander, A.I., and Rowe, T.B. 2022. Reexamination of the mandibular and dental morphology of the Early Jurassic mammaliaform *Hadrocodium wui*. *Acta Palaeontologica Polonica* 67 (1): 95–113.

CT visualization of the mandible and dentition of *Hadrocodium wui*, a stem mammaliaform from the Lower Jurassic Lower Lufeng Formation of Yunnan, China has revealed new features not accessible by previous microscopic study of the fossil. Its mandible shows a postdentary trough with an overhanging medial ridge and a short Meckel's sulcus. An incomplete part of the ectotympanic and possibly a remnant of Meckel's element are preserved in the postdentary trough. Thus, *Hadrocodium* is similar to other mammaliaforms in retaining a mandibular middle ear, contrary to our earlier interpretation. The mandible exhibits a large postcanine diastema from shedding of anterior premolars without replacement, an age-dependent feature better developed in older adults. Another adult feature is the alignment of the ultimate molar to the coronoid process. This is consistent with age-dependent changes in other mammaliaforms where the last molars of the toothrow shift from medial of the coronoid process in the juvenile, to a position in front of the coronoid process in the adult. The mandible has a short mobile symphysis. The dentition consists of I5, C1 (two-rooted), P3 (including P1 position) and M2 (M2 with confluent roots), and i4, c1 (partially two-rooted), p3, and m2 (m2 with partially confluent roots). The two-rooted upper canines are more derived than other Early Jurassic mammaliaforms from the same fauna, although similar to docodontans. *Hadrocodium* is unique in that the lower m2 cusp a occludes in the embrasure between upper M1–M2, but the posterior part of m2 shows between-cusp occlusion with upper M2 main cusp A. M2 is half the size of the lower m2, and occludes only with the distal half of m2. The upper postcanines show a steep gradient of posteriorly decreasing tooth size, more so than other mammaliaforms. The CT examination corroborates that there are no unerupted teeth in the upper or lower jaws, and the holotype of *H. wui* is dentally and osteologically mature and capable of independent feeding.

Key words: Mammaliaformes, *Hadrocodium*, dental morphology, growth pattern, Jurassic, China.

Zhe-Xi Luo [zxluo@uchicago.edu; ORCID 0000-0003-2170-8879] and April I. Neander [aisch@uchicago.edu; ORCID 0000-0001-6816-2872], Department of Organismal Biology and Anatomy, University of Chicago, 1027 East 57th Street, Chicago, Illinois 60637, USA.
Bhart-Anjan S. Bhullar [bhart-anjan.bhullar@yale.edu; ORCID 0000-0002-0838-8068], Department of Earth and Planetary Sciences and Peabody Museum of Natural History, Yale University, New Haven, Connecticut 06511, USA.
Alfred W. Crompton [acrompton@oeb.harvard.edu; ORCID 0000-0001-6008-2587], Museum of Comparative Zoology, Harvard University, Cambridge, Massachusetts 02138, USA.
Timothy B. Rowe [rowe@utexas.edu; ORCID 0000-0002-8869-4582], Jackson School of Geosciences and High-Resolution X-ray Computed Tomography Facility, University of Texas at Austin, Austin, Texas 78712, USA.

Received 1 October 2021, accepted 2 March 2022, available online 30 March 2022.

Introduction

Hadrocodium wui (Luo et al. 2001) is a stem mammaliaform from the Lower Jurassic of China. It is characterized foremost by an expanded braincase with a large brain endocast volume relative to its small skull size, overlapping with the range of brain encephalization of crown Mammalia (Rowe et al. 2011). Given its basal position in mammaliaform phylogeny, characteristics of *Hadrocodium* have broader ramifications for understanding the morphological transformation through the descent of mammals from the non-mammaliaform cynodonts (Luo 2007; Rowe and Shepherd 2016; Lautenschlager et al. 2018). In some large-scale phylogenetic studies of mammals, *H. wui* was included

as a comparative taxon for overall interpretation of mammaliaform phylogenies (e.g., Luo et al. 2002, 2017; O'Meara and Thompson 2014; Bi et al. 2014; Zhou et al. 2019). For other studies this fossil was also used as sister taxon for crown Mammalia, and for time-calibration of the mammalian family tree (Tarver et al. 2016; Liu et al. 2017). Its morphologies have been used in other studies on evolution of the brain and cranial muscles (Rowe and Shepherd 2016; Laaß and Kaestner 2017; Lautenschlager et al. 2017, 2018; Rowe 2020).

Hadrocodium wui is a very small mammaliaform. Measured at 12 mm in skull length, it approaches the size range of the smallest-known mammals from the Cenozoic (Bloch et al. 1978; Gebo et al. 2000; Jürgens 2002). It is well established that the evolution from non-mammaliaform cynodonts to modern mammals went through a transformative phase of miniaturization (reduction of body size) with the earliest mammaliaforms (Lautenschlager et al. 2018). *Hadrocodium* is a major taxon that exemplifies this large-scale evolutionary pattern. The initial systematic paleontology study (Luo et al. 2001) was based on traditional mechanical preparation of the fossil in 1992–1993. Although the skull of *H. wui* was scanned by Computed Tomography (CT) in 2003, which resulted in studies of its brain endocast (Macrini 2006; Rowe et al. 2011), the rest of the skull has yet to be analyzed from these CT data. Here we provide a detailed description of the mandibles and the teeth from reexamination of this fossil by CT scans, which revealed new information unavailable from previous fossil preparation. This helps to correct some inaccurate interpretations of ours on the mandibular structure and the middle ear (Luo et al. 2001; Luo 2011), as well as the dental occlusal pattern.

Institutional abbreviations.—BMNH, Beijing Museum of Natural History, China; CUP-FMNH, Field Museum of Natural History-Catholic University of Peking collection, Chicago, USA; DMNH, Dalian Museum of Natural History, Dalian, Liaoning, China; IVPP, Institute of Vertebrate Paleontology and Paleoanthropology, Chinese Academy of Sciences, Beijing, China; MCZ, Museum of Comparative Zoology, Harvard University, USA; Gui-Mam, Guimarota mammal fossils, currently housed for study at Institute for Geosciences, Section of Paleontology of the University of Bonn, Germany (the Gui Mam collection belongs to the paleontological collection of the Serviços Geológicos de Portugal, Lisboa, Portugal); UMZC, University Museum of Zoology Cambridge, Cambridge University, UK; YPM, Yale Peabody Museum of Natural History, New Haven, USA.

Other abbreviations.—We follow standard convention in abbreviating tooth families as I, C, P, and M, with upper and lower case letters referring to upper and lower teeth, respectively.

Material and methods

The holotype specimen of *Hadrocodium wui* (IVPP 8275) was discovered by Xiao-Chun Wu in 1985 near the Dadi locality of the Lufeng Basin, of Yunnan Province, China. The fossil was from the Upper Red Beds of the Lower Lufeng Formation, estimated to be Early Jurassic in age (Sinemurian, about 195 million years) by faunal correlation (Luo and Wu 1994; Kielan-Jaworowska et al. 2004). The specimen was hand-prepared from 1992 to 1993 by the late William W. Amaral, the fossil preparator of the Museum of Comparative Zoology at Harvard University (Cambridge, USA). After the initial study of *H. wui* (Luo et al. 2001), the type specimen was scanned in 2003 by Rich Ketcham at the CT Lab at the High-Resolution Computed Tomography Facilities in University of Texas (Austin, USA), on the ACTIS scanner with detector panel of 1024 × 1024 dpi, at 150 kv and 0.38 mA. The scan resolution is 0.0191 mm in slice thickness, and also 0.0191 mm in inter-slice spacing.

The dataset used here for studying the teeth and mandible is the same dataset as for the Rowe et al. (2011) study on the brain endocast of *H. wui*. The segmentation and image analyses from the CT data were completed by co-author AIN using the software Mimics (www.materialise.com) in the Department of Organismal Biology and Anatomy of the University of Chicago.

Systematic palaeontology

Mammaliaformes Rowe, 1988

Genus *Hadrocodium* Luo, Crompton, and Sun, 2001

Type species: *Hadrocodium wui* Luo, Crompton, and Sun, 2001; see below.

Hadrocodium wui Luo, Crompton, and Sun, 2001

Fig. 1.

Holotype: IVPP 8275, a nearly complete skull.

Type locality: Dadi Locality, Lufeng Basin, Yunnan Province, China.

Type horizon: Upper Red Beds of the Lower Lufeng Formation, Lower Jurassic.

Material.—IVPP 8275 holotype.

Emended diagnosis.—Dental formula I5/i4 C1/c1 P3/p3 M2/m2. It differs from species of *Morganucodon*, *Erythrotherium*, *Dinnetherium*, *Haldanodon*, and triconodontids in that primary lower cusp a occludes in the embrasure between the opposite upper molars, instead of the primary cusp a of the lower molar m2 occluding between cusps A and B of the upper M1 and M2. It differs from *Megazostrodon rudnerae* Crompton and Jenkins, 1968, in lacking prominent labial cingulid cuspules of the upper and from kuehneotheriids in lacking the triangulation of molar cusps. It differs from morganucodontids, eutriconodonts, and kuehneotheriids in the presence of a much larger postcanine diastema. It differs from

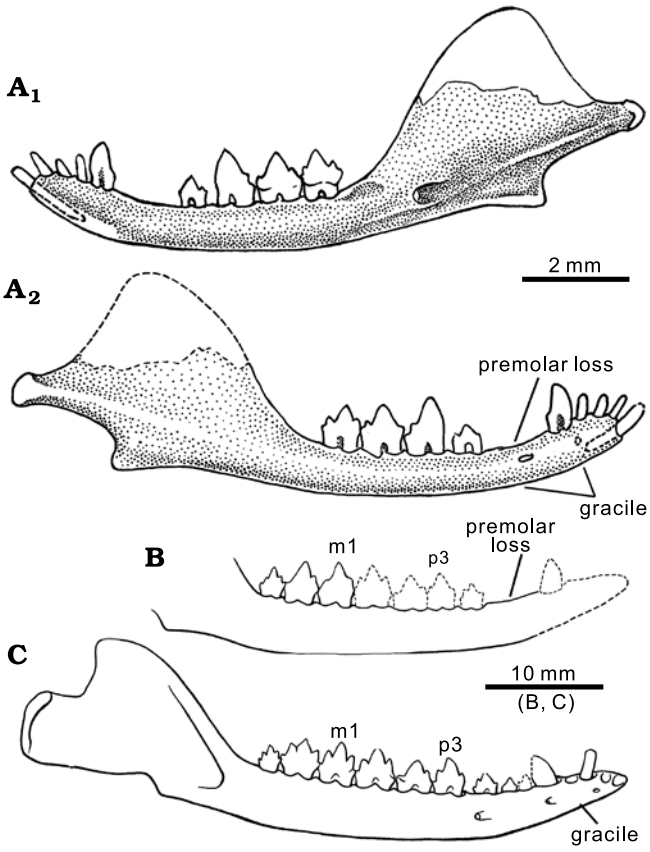

Fig. 1. Lower jaws of comparative mammaliaforms. **A**. *Hadrocodium wui* Luo, Crompton, and Sun, 2001 (holotype, IVPP 8275), from the Lower Lufeng Formation, Lower Jurassic of Yunnan, China. Right mandible in lingual (A_1) and labial (A_2) views. **B**, **C**. Morganucodontan *Dinnetherium nezorum* Jenkins, Crompton, and Downs, 1983, from the Kayenta Formation, Lower Jurassic of Arizona, USA. **B**. An older adult (MCZ 20910). **C**. A young adult (MCZ 20870); modified from Crompton and Luo 1993). Younger individuals of *D. nezorum* have a full set of five premolars, while older individuals have lost up to two anterior premolars without replacement. The postcanine diastema developed by shedding premolars without replacement is an aging-related character of many mammaliaforms including *Hadrocodium*.

Sinoconodon and most cynodonts in the one-to-one precise occlusion of the upper and lower molars. It lacks the multicuspate rows on the teeth of *Haramiyavia clemmenseni* Jenkins, Gatesy, Shubin, and Amaral, 1997, *Kalaallitkigun jenkinsi* Sulej, Krzesiński, Tałanda, Wolniewicz, Błażejowski, Bonde, Gutowski, Sienkiewicz, and Niedźwiedzki, 2020, multituberculates, and the multiple-ridged teeth of docodonts.

Description.—Mandibles: The mandibular body (alveolar ramus) is gracile and dorso-ventrally shallow. Its ventral margin is slightly convex, and the tooth-bearing alveolar margin is straight along the postcanine row but noticeably curved upward in the postcanine diastema anterior to the first preserved premolar, and in the symphyseal region of the mandible. The symphyseal region of the mandible is even thinner than the diastema region and the mandibular body along the tooth row (Figs. 1–3). The gracile nature of the mandibular part that bears incisors and canine suggests that there might have been bone resorption after the loss of the anterior premolars. The ventral margin of this mandibular part was slightly damaged by abrasion before the specimen was found. Due to the abrasion, the roots of incisors and canine are partly exposed (Figs. 2–4).

The postcanine diastema is a pronounced feature between the canine and the first preserved premolar, herein designated as p2. Anterior to the p2 there are two dimples on the dorsal margin of the mandible, which clearly represent the plugged alveoli of a two-rooted premolar that was shed at this locus. These plugged (although clearly recognizable) alveoli suggest that there used to be an anterior premolar (p1) in this position. It cannot be ruled out that the postcanine diastema may have accommodated more than one premolar. But here we offer a conservative estimate that *H. wui* has three premolar positions, and we designate the lost premolar represented by the two plugged alveoli to be p1 (see Discussion).

The coronoid process rises from the alveolar line of the mandibular body, forming a 120–125° angle to the anterior border of the coronoid (Figs. 1–3). The fully developed dentary condyle is preserved on the right mandible, but broken on the left mandible. The condyle is differentiated from the posterior part of the coronoid process by a constricted peduncle, a structure typical of stem mammaliaforms, including haramiyidans (Luo et al. 2002; Gill et al. 2014; Luo et al. 2015a; Schultz et al. 2019; Panciroli et al. 2019; Sulej et al. 2020). The condyle is slightly compressed dorsoventrally, less robust than the more bulbous and rounded dentary condyles of *Morganucodon* species (Kermack and Mussett 1958; Kermack et al. 1973; Gill et al. 2014) and *Sinoconodon rigneyi* Patterson and Olson, 1961 (Crompton and Sun 1985; Crompton and Luo 1993; Luo 1994; Luo and Wu 1994; Luo et al. 1995).

The anterior margin of the coronoid process is aligned mesio-distally with the postcanine row (including m2). Between the ultimate molar (m2) and the rising base of the coronoid process there is a gap, herein called the retro-molar space (Figs. 3 and 4: arrow). We interpret that the direct alignment of the toothrow in front of the coronoid process is an adult feature, by comparison to the adult pattern of other mammaliaforms with more complete series of ontogenetic stages, and this feature is also apomorphic in a phylogenetic context (details in Discussion).

Lingual aspect: The mandibular symphysis is marked by a distinct area on the lingual aspect of the anterior part of the mandible. Although the symphyseal surface is somewhat damaged on both mandibles, the preserved parts of symphysis show that it is slightly rugose. As preserved, the two hemimandibles are not in direct contact, indicating that the mandibular symphysis was connected by soft tissues that are not fossilized (Figs. 1–3). The symphysis extends posteriorly to below the canine, and this posterior extent of the symphysis is much shorter than the symphyses that extend to the level of the p3 in species of *Morganucodon*, or to the ultimate premolar (p5) or m1 in docodontans. We

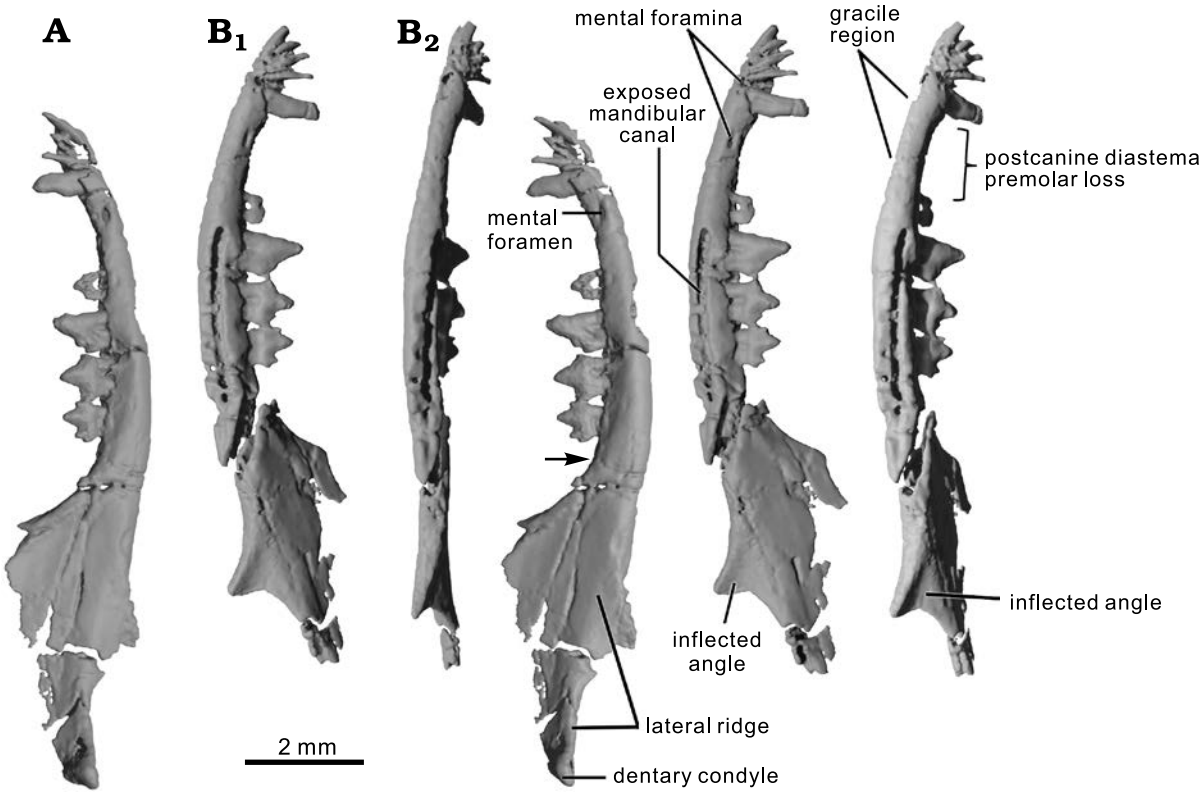

Fig. 2. CT rendering of the mammaliaform *Hadrocodium wui* Luo, Crompton, and Sun, 2001 (holotype, IVPP 8275) from the Lower Lufeng Formation, Lower Jurassic of Yunnan, China. **A**. Right mandible in lateral view (stereopairs); solid triangle indicates the retro-molar space. **B**. Left mandible in lateral (B_1, stereopairs) and ventral (B_2, stereopairs) views.

interpret that the symphyseal contact likely was mobile, as in all known mammaliaforms, and a vast majority of crown mammals (Kielan-Jaworowska et al. 2004; Scott et al. 2012).

The Meckel's sulcus is present in the molar region of the mandibular body (Figs. 1–3). The sulcus is short, and extends from below the foramen of the mandibular canal anteriorly toward the ventral mandibular margin; its anterior end fades out below the ultimate molar (m2). However, there is no Meckel's sulcus on the lingual side of the mandible between the symphysis and the posterior premolars, which is confirmed on the scan slices. The Meckel's sulcus is present in the premolar and symphyseal region in juvenile or young adult individuals of other mammaliaforms. For example, the Meckel's sulcus is present in this region in juvenile growth stages of species of *Morganucodon*, *Docodon*, and *Haldanodon* but the sulcus disappears in this region in full adult specimens of the same taxa (Kermack et al. 1973; Krusat 1980; Schultz et al. 2019; see also adult mandible of *Borealestes serendipitus* Waldman and Savage, 1972; Panciroli et al. 2019).

The postdentary trough is present on the medial side of the mandible, and a part of this trough is dorsally bordered by the medial ridge (Figs. 1–3). The trough is shallow along its entire length and its anterior part contains the mandibular foramen. Posterior to the foramen the trough is open dorsally and lacks a border, likely for the passage of the inferior alveolar nerve (from the mandibular branch of the trigeminal nerve) into the mandibular canal. The posterior end of the trough becomes slightly wider and opens in a shallow embayment posteriorly below the posterior part of the medial ridge (Figs. 1–3).

Some incomplete parts of middle ear elements are detected by CT scans, and can be visualized (Fig. 4). The preserved parts certainly include a part of the ectotympanic (or "angular") bone. Another preserved element may be a fragment of the Meckel's element (or the "prearticular"). However, the surangular as interpreted for *Morganucodon oelheri* Rigney, 1963, by Kermack et al. (1973), cannot be identified with certainty. The identities of these postdentary elements are difficult to establish and remain uncertain due to poor preservation. These elements cannot be fully resolved until better specimens of *H. wui* are recovered in the future.

On the medial side and near the base of the coronoid process, there is an oval and elongate depression, which we interpret to be the coronoid facet. Near the coronoid fossa of the right mandible, a small piece could belong to the coronoid bone but this identification remains tentative because this element is difficult to trace in coronal CT slices, and must be corroborated by additional specimens of *H. wui* recovered in the future. Although smaller, the fossa for the coronoid is identical in shape and position to the coronoid facet of *Morganucodon watsoni* Kühne, 1949 (Kermack et al. 1968). The coronoid fossa is less similar to that in *Kuehneotherium praecursoris* D.M. Kermack, K.A. Kermack, and Mussett, 1968 (Gill 2004; Gill et al. 2014) than to *M. watsoni* (Pamela Gill, personal communication 2021).

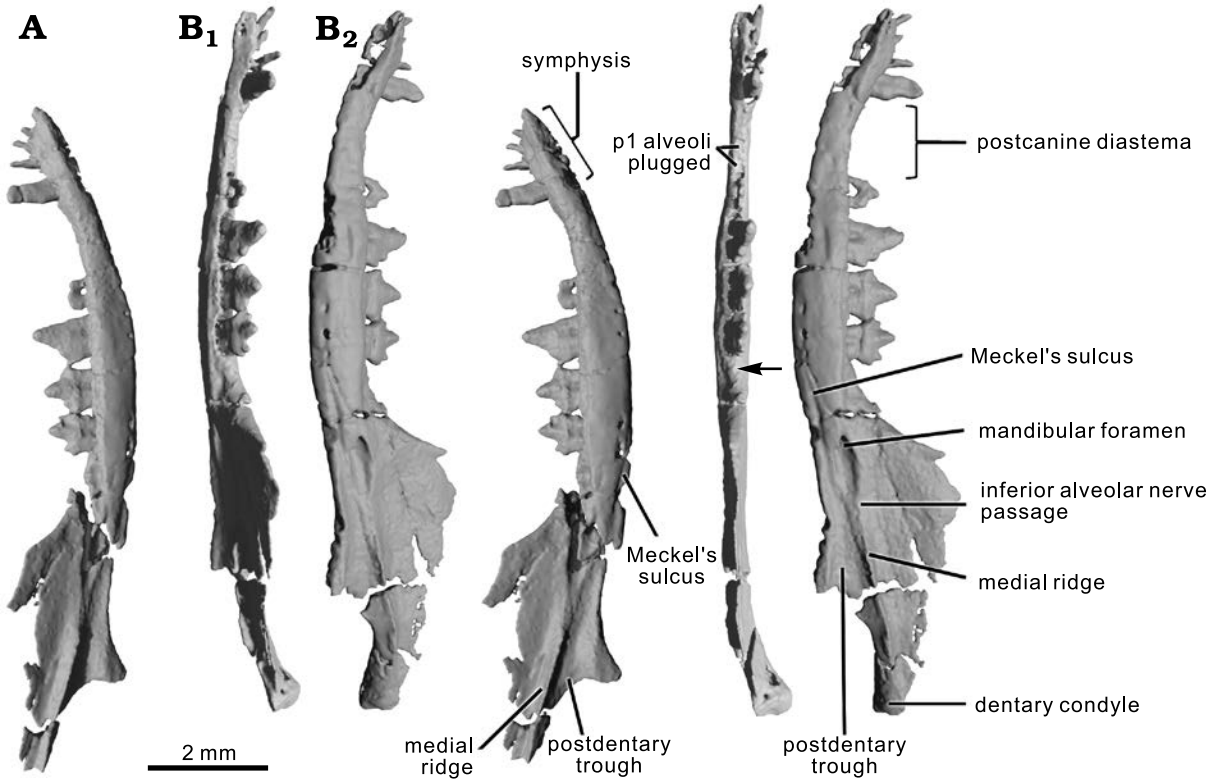

Fig. 3. CT rendering of the mammaliaform *Hadrocodium wui* Luo, Crompton, and Sun, 2001 (holotype, IVPP 8275) from the Lower Lufeng Formation, Lower Jurassic of Yunnan, China. **A**. Left mandible in medial view (stereopairs). **B**. Right mandible in tilted dorsal view (B_1, stereopairs), p1 is lost but the p1 position is indicated by plugged alveoli; arrow indicates the retro-molar space; and medial view (B_2, stereopairs).

Hadrocodium shares plesiomorphic features related to the postdentary trough with basal mammaliaforms. Notwithstanding the minor differences of a shorter and thinner Meckel's sulcus, a shallower trough, and much weaker medial ridge, *Hadrocodium* shares these plesiomorphic features with *Sinoconodon*, morganucodontans, and docodontans. This new revelation by CT scanning necessitates a major revision of the interpretation of these features by Luo et al. (2001).

The alveolar margin of the mandible is nearly straight and horizontal. The posterior part of this margin lacks the dental lamina groove (Crompton's groove sensu Parrington 1971); this groove is a plesiomorphic feature present in species of *Morganucodon* and *Sinoconodon rigneyi*, and a wide range of non-mammaliaform cynodonts on the lingual side near the last molars (Kermack et al. 1973; Crompton and Luo 1993). The absence of this feature is an apomorphy of *Hadrocodium* and is otherwise known in docodontans (Schultz et al. 2019; Panciroli et al. 2019) and in the Late Triassic haramiyidans (Jenkins et al. 1997; Luo et al. 2015a; Sulej et al. 2020).

Labial aspect: On the labial side of the mandible, the coronoid process has a shallow concave area, identified as the masseteric fossa. The anterior border of the fossa lacks a distinct border and grades into the mandibular body as in species of *Morganucodon* (Kermack et al. 1973; Crompton and Luo 1993; Lautenschlager et al. 2017). The ventral extent of the masseter muscle attachment is not a clearly demarcated border in *H. wui*; this is similar to *Dinnetherium nezorum* Jenkins, Crompton, and Downs, 1983 (Jenkins et al. 1983; Crompton and Luo 1993) and to docodontans (Krusat 1980; Ji et al. 2006; Schultz et al. 2019; Panciroli et al. 2019). There is no foramen in the masseteric fossa, as in some derived zatherian mammals (Davis 2012). The lateral ridge extending from the dentary condyle and peduncle is distinctive. We interpret that the lateral ridge is a landmark boundary, approximately, between the concave surface for M. masseter profundus dorsally and a narrow, flat surface for the M. masseter superficialis on the moderately inflected angular process of the mandible, as reconstructed for other mammaliaforms, by comparison to extant mammals (Turnbull 1970; Lautenschlager et al. 2017; Schultz et al. 2019).

Two mental foramina are present on the labial side of the anterior (symphyseal) part of the mandible (Figs. 1–3). The anterior of these foramina is small and located between i4 and the canine on the better preserved left mandible. The posterior mental foramen is oval shaped and much larger than the anterior-most foramen. It is located in the postcanine diastema region on both mandibles, just anterior to the level of the p1 position indicated by plugged alveoli of this tooth. These foramina are connected to the mandibular canal inside the mandibular body (Fig. 5).

The mandibular canal on the left mandible is exposed by erosion of the thin cortical bone. From the exposed width of the canal, and from the cross section of the right mandible, the canal diameter is measured to be 0.12–0.13 mm, in a mandibular body that is 0.8–0.9 mm in height (Figs. 2, 5).

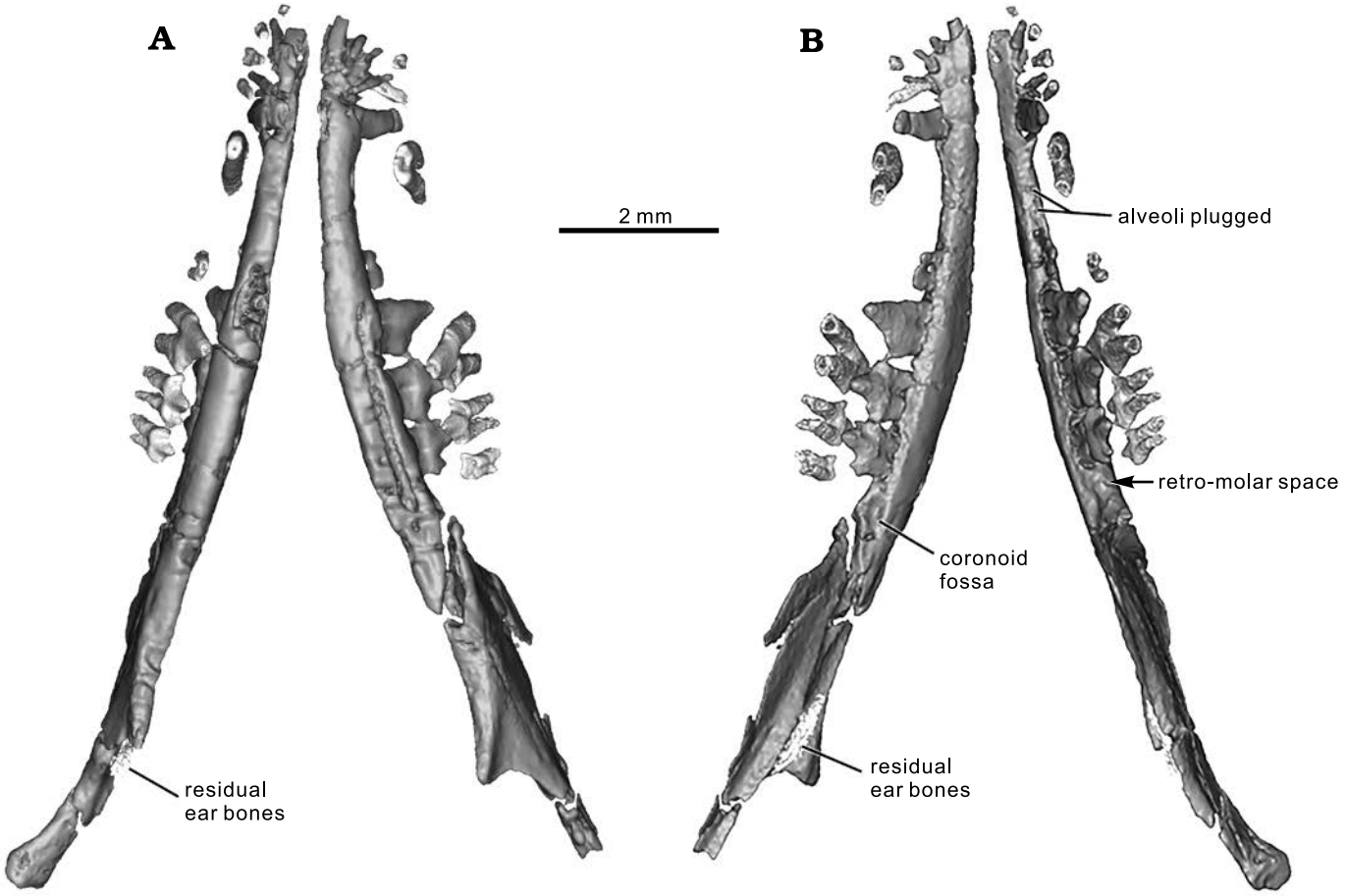

Fig. 4. CT rendering of the mammaliaform *Hadrocodium wui* Luo, Crompton, and Sun, 2001 (holotype, IVPP 8275) from the Lower Lufeng Formation, Lower Jurassic of Yunnan, China. **A**. Mandibles and upper teeth (as preserved) in ventral view. **B**. Mandibles in association with upper teeth in dorsal view. The upper teeth are more inclined (as preserved) and are oblique to the lower teeth. Post-mortem distortion caused the upper postcanines to shift relative to lower teeth, by half a cusp length.

The canal is oval in cross section (Fig. 5) and is similar in *H. wui* and *M. oehleri*. The canal is positioned lateral to the root alveoli in cross section and is in the laterally bulging part of the mandibular body (Fig. 5A). The lateral placement of this canal relative to the postcanine alveoli is similar in *H. wui* and *M. oehleri*, but this placement is slightly different from the canal's position in docodontans. In all docodontans examined so far (Schultz et al. 2019; Panciroli et al. 2019), the mandibular canal is ventrolateral to the tooth root apices (Fig. 5C, D). The latter pattern of docodontans is more closely comparable to those of extant therians than in morganucodontans and *Hadrocodium*, and therefore more derived. In crown mammals of the Mesozoic, such as the eutriconodontans *Juchilestes* and *Repenomamus*, the mandibular canal is located directly ventral to the root apices (Fig. 5E).

The mandibular canal diameter is 14.5 to 15% the size of the mandibular body depth. If scaled to the width or the lingual side depth (= height) of the mandibular body, the mandibular canal shows about the same proportion to the width and height of the mandibular body (Fig. 5) as the canals of docodontans and morganucodontans. The mandibular body of *H. wui* shows a distinct pattern in that the height of the mandibular body is lower on the labial side of the postcanine alveoli (Fig. $5A_2$: asterisk), than on the lingual side of the alveoli (Fig. 5: arrow). The mandibular canal diameter appears to be slightly larger if it is scaled to the labial height of the mandible. Overall, the mandibular canal diameter is about the same relative to the mandibular body in *H. wui*, as in species of *Morganucodon* and docodontans. The mandibular canal of mammaliaforms (including *H. wui*) is much smaller than those of Cretaceous *Teinolophos trusleri* Rich, Vickers-Rich, Constantine, Flannery, Kool, and Van Klaveren, 1999, and the extant monotremes, than previously interpreted by Rowe et al. (2008).

Dentition: Here we are revising the dental formula of *H. wui* to I5/i4–C1/c1–P3/p3–M2/m2 (Figs. 6–9). This change includes the alveoli of the first upper and lower premolars that were shed in the P1/p1 position. The new formula differs from the previous I5/i4–C1/c1–P2/p2–M2/m2 (Luo et al 2001: fig. 1), but the previous study only counted the intact permanent teeth and excluded the upper P1 and lower p1 positions indicated by the visible (but plugged) alveoli of the shed premolars. In the following description we use a dental formula that includes the tooth positions represented by empty and plugged alveoli. We also follow

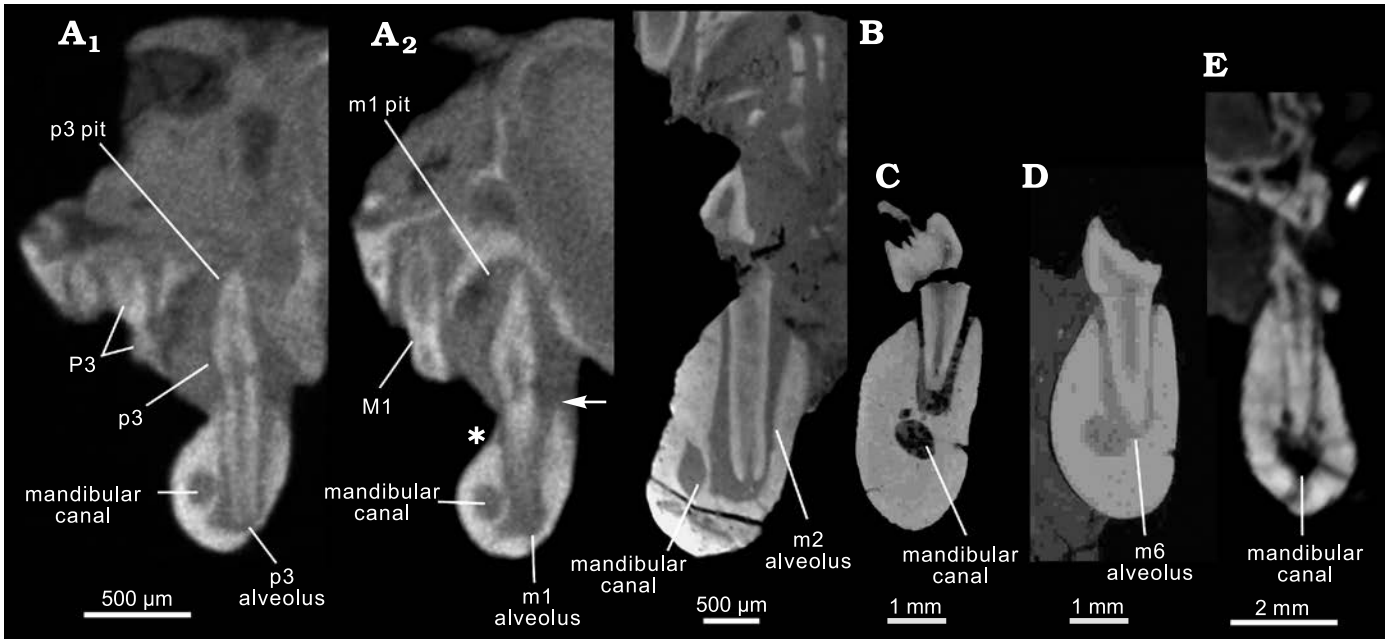

Fig. 5. Comparative morphology of mandibular canals and tooth alveoli in cross sections. **A**. The mammaliaform *Hadrocodium wui* Luo, Crompton, and Sun, 2001 (holotype, IVPP 8275) from the Lower Lufeng Formation, Lower Jurassic of Yunnan, China; transverse section of mandible through anterior root of p3 (A_1): the main cusp of a tall p3 occludes into its maxillary pit on the palate, and the upper P3 is more lingually inclined than the lower p3; transverse section through anterior root of m1 (A_2): the mandibular canal is lateral to the root alveoli of the postcanines; the upper M1 is more inclined lingually than the lower m1; the main cusp of lower m1 occludes into its pit on the palate; the asterisk indicates that the labial alveolar margin is lower on the lingual alveolar margin at the point of the arrow. **B**. The morganucodontan *Morganucodon oehleri* Rigney, 1963, (BMNH 2858) from the Lower Lufeng Formation, Lower Jurassic of China; cross section through the anterior root of m2: oval outline with long diameter at 0.25 mm, and short diameter at 0.15 mm; mandibular canal is lateral to the side of roots. **C**, **D**. The docodontan *Docodon victor* Schultz, Bhullar, and Luo, 2019 (as revised by Schultz et al. 2019) from the Morrison Formation, Upper Jurassic of Wyoming, USA. **C**. YPM 11826, cross section through a root alveolus of m5; mandibular canal cross section in oval outline with the long diameter at 0.8 mm and short diameter at 0.6 mm. **D**. YPM 11823, mandibular canal cross section through anterior root of m5; circular outline diameter 0.6 mm. The mandibular canal is ventro-lateral to the apices of roots in docodontans. **E**. The eutriconodontan *Juchilestes liaoningensis* Gao, Wilson, Luo, Maga, Meng, and Wang, 2009 (DMNH 2607) from the Yixian Formation, Lower Cretaceous of China, as a representative for root canal pattern for crown mammals, in which the mandibular canal is ventral to the root apices.

Crompton and Jenkins (1968) and Crompton (1974) for their scheme of cusp designations.

Upper dentition: There are five upper incisors in the better-preserved right premaxilla (Luo et al. 2001; Rowe et al. 2011). Crowns of I2–I4 are intact but I1 and I5 are broken, although their alveoli can be clearly identified (Figs. 6, 7, 9). The left premaxilla has preserved only I4 (incomplete) and I5; the left I1–I3 and their corresponding left premaxillary part are damaged and lost. The I5 is separated from the upper canine by a gap that accommodates the tall and trenchant lower canine locking into a deep canine pit (the paracanine fossa) in the premaxilla when in full occlusion (Fig. 6). This is visible from cross sections of the CT scans.

The upper canine shows a triangular outline in lateral profile and is slightly compressed medio-laterally (Figs. 6, 7, 9). The canine has two strong roots divergent from each other at an angle of 20–25°. The conical shape of the crown as previously illustrated by Luo et al. (2001: fig. 1) was not correct. The posterior root of the two divided roots was not detected by manual fossil preparation in previous study (Luo et al. 2001), as the root was covered by a mixture of frail bone and matrix in the specimen. The upper postcanine diastema is a prominent gap between the two-rooted canine and the preserved premolars (P2 and P3 on the right side, but only P3 on the left side). The right maxillary alveolar margin in the postcanine diastema shows a surface dimple corresponding to a single plugged alveolus (Fig. 6). This is identified by CT visualization, and also recognizable on the specimen under the microscope. This plugged alveolus is interpreted to have held a single-rooted premolar that was shed. Its position is herein designated as "P1-position" (Figs. 5–7).

The upper P2 is preserved only on the right maxilla, but this tooth on the left maxilla was lost without being replaced, and its two alveoli are plugged though still recognizable. The right P2 is two-rooted but its crown is broken. The tooth is separated anteriorly from the plugged P1 alveolus by a small interdental gap. It is also separated posteriorly from P3 by a very small interdental gap. P3 is the largest of all teeth in height and in length (Table 1). Its large main cusp (cusp A) is slightly asymmetrical with a straight anterior crest and a slightly concave posterior crest. At the cingular level, the tooth shows no distinctive cingular line on either the lingual or the labial aspect although in the cingular positions there are slight bulges. There are two miniscule cingular cuspules on the mesial and the distal ends of the crown. However, the

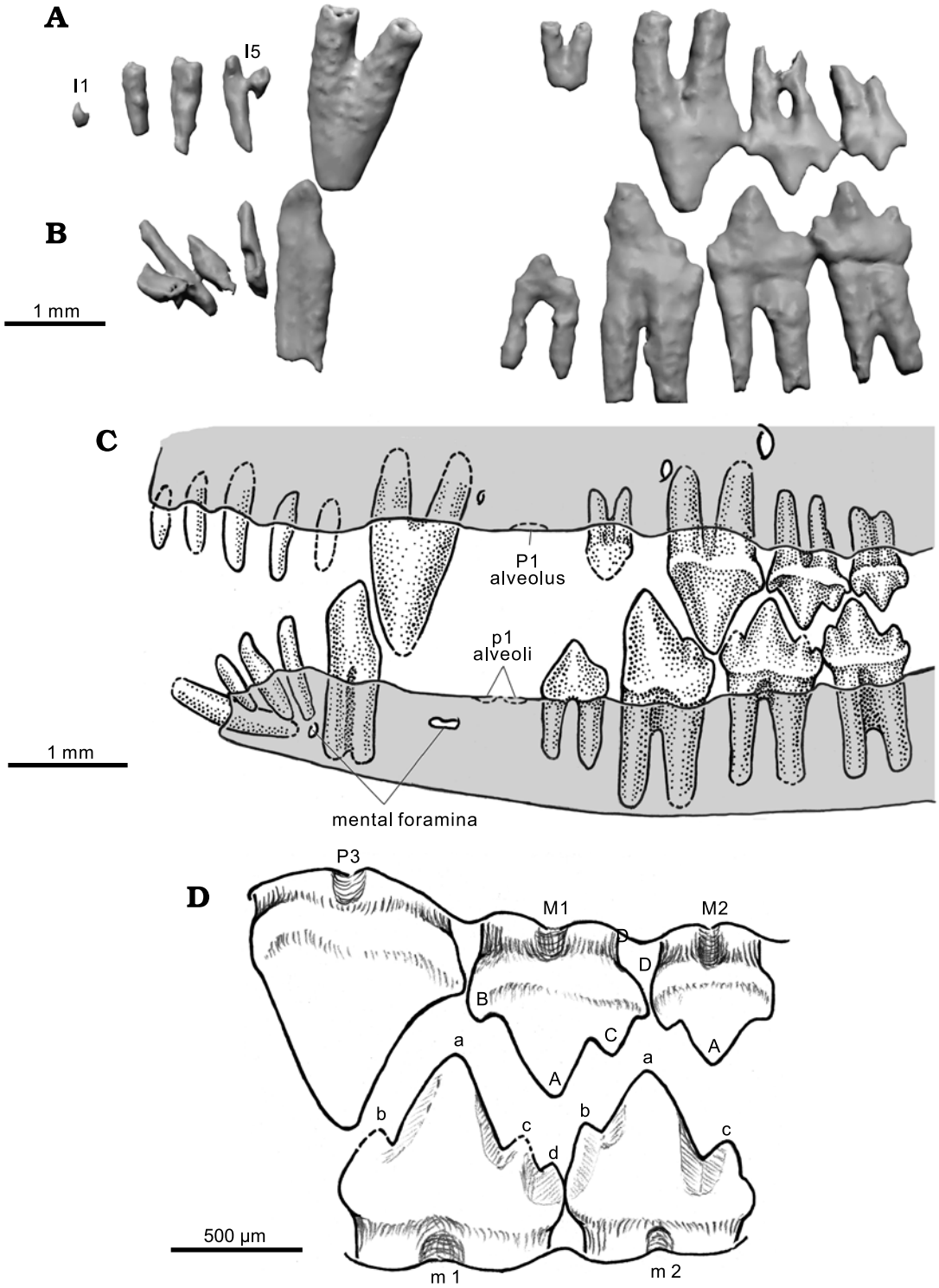

Fig. 6. Composite reconstruction of full dentition of *Hadrocodium wui* Luo, Crompton, and Sun, 2001 (holotype, IVPP 8275) from the Lower Lufeng Formation, Lower Jurassic of Yunnan, China. **A**. Left upper teeth (as preserved) in labial view (CT visualization). **B**. Lower teeth (as preserved) in lingual view. **C**. Composite reconstruction of upper and lower teeth (left labial view). **D**. Occlusal relationship of cusps between lower m1–m2 and upper P3–M1–M2 (revised from Luo et al 2001: fig. 1; cusp designation following Crompton and Jenkins 1968 and Crompton 1974).

large mesial cuspule illustrated in previous study (Luo et al. 2011: fig. 1) is an artefact, as shown by CT visualization. The left and right P3s show an asymmetrical variation on two sides: the left P3 has a weakly developed cusp on the posterior crest, which is entirely absent on the right P3 (Fig. 7). We could not rule out that this difference is caused by preservation differences of the left P3 versus the right P3.

The upper M1 is better preserved on the right side than the left. This tooth bears three main cusps: the primary cusp A in the middle, a lower but pointed cusp B on the mesial

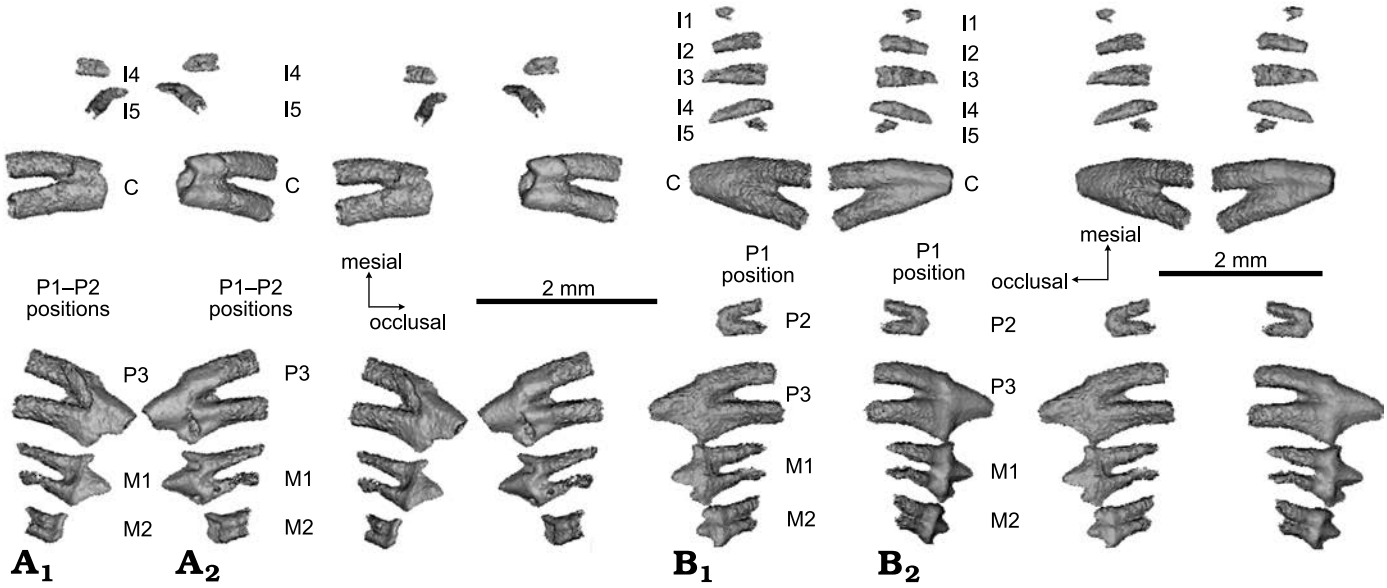

Fig. 7. CT rendering of mammaliaform *Hadrocodium wui* Luo, Crompton, and Sun, 2001 (holotype, IVPP 8275) from the Lower Lufeng Formation, Lower Jurassic of Yunnan, China. **A**. Left upper teeth (as preserved and virtually extracted from the upper jaws): incomplete incisors, canine, incomplete premolars and two molars in lingual (A_1, stereopairs) and labial (A_2, stereopairs) views. Left dentition has five incisor positions: two broken incisors, plus three additional incisors represented by alveoli visible on the fossil skull (but not visualized in teeth). Of the three premolars, P1 is not preserved, but P1 position is represented by a plugged alveolus on right side (not visualized here). P2 is preserved on right side, but is lost and represented only by empty alveoli on the left. P3 is intact on both sides. **B**. Right upper teeth: five upper incisors (I1 and I5 broken), canine, two premolars, two molars in lingual (B_1, stereopairs) and labial (B_2, stereopairs) views.

end of the crown, and a low posterior cusp C (worn off on the left M1). Additionally, a miniscule cingular cusp D is on the distal end of the crown (Figs. 6, 7). The base of the crown has a slightly bulging labial cingulum although lacking any cingular line or cuspules. The lingual aspect of the tooth exhibits a weak cingulum, which is otherwise featureless. M1 has two fully divided roots and the posterior root is curved or slanted mesially, in both the left and the right M1. The distal part of left M1 appears to be either heavily worn or damaged in fossilization, such that cusp C and cuspule D are lost.

Table 1. Dental measurements (in mm) of the holotype of the mammaliaform *Hadrocodium wui* (IVPP 8275) from the Lower Lufeng Formation, Lower Jurassic of China. [1] measurement of width across the primary cusp a; [2] measurement of height from below crown base at the depression of root junction to the apex of primary cusp a; * right p3 length is incomplete because anterior margin of the crown is slightly damaged.

Right upper teeth	P3	M1	M2
length	0.8	0.67	0.47
width[1]	0.3	0.27	0.27
height[2]	0.8	0.48	0.37
Left lower teeth	p3	m1	m2
length	0.75	0.84	0.7
width[1]	0.25	0.24	0.24
height[2]	0.92	0.62	0.59
Right lower teeth	p3	m1	m2
length	0.72*	0.82	0.73
width[1]	0.23	0.28	0.26
height[2]	0.8	0.82	0.65

M2 is characterized by the taller cusp A and shorter cusps B and C located respectively at the mesial and distal ends of the crown. But it lacks distal cuspule D. The tooth crown is antero-posteriorly symmetrical with respect to the middle cusp A. M2 has two fully confluent roots connected by dentine over the root length. The M2 roots are much shorter than those of M1. The gradient of variation of the successively more confluent and shorter roots in the more posterior molars, as seen here in *H. wui* (Fig. 7), is also well documented in specimens of *Morganucodon watsoni*, in which the last upper molar (M4) has the smallest (also the shortest) crown of all postcanines, and often with a fusion of the two roots (Parrington 1971; Kermack et al. 1981; Jäger et al. 2019). The upper molars of *Kuehneotherium praecursoris* also show a gradient of variation in root fusion of molars (Mills 1984; Gill 2004). In the latest reconstruction of the toothrow in *Kuehneotherium praecursoris*, Gill (2004) placed the smaller to smallest upper molars with more fused roots in the ultimate toothrow position(s), although the degree of fusion of the two roots can be variable in the posterior molars (Gill 2004, personal communication 2021).

The upper M2 is very small, its crown is much shorter than the M1 crown, and lower in height than P3 and M1 (50% of P3 length and 65% of the M1 length). Taken together, P3, M1, and M2 form a posteriorly decreasing size (length) and height gradient. The posteriorly decreasing size of molars is also present between m2 and the ultimate molar (m4 or m5) in morganucodontans and docodontans, but the steep gradient of size reduction in P3–M1–M2 is an unusual and distinct feature of *H. wui*.

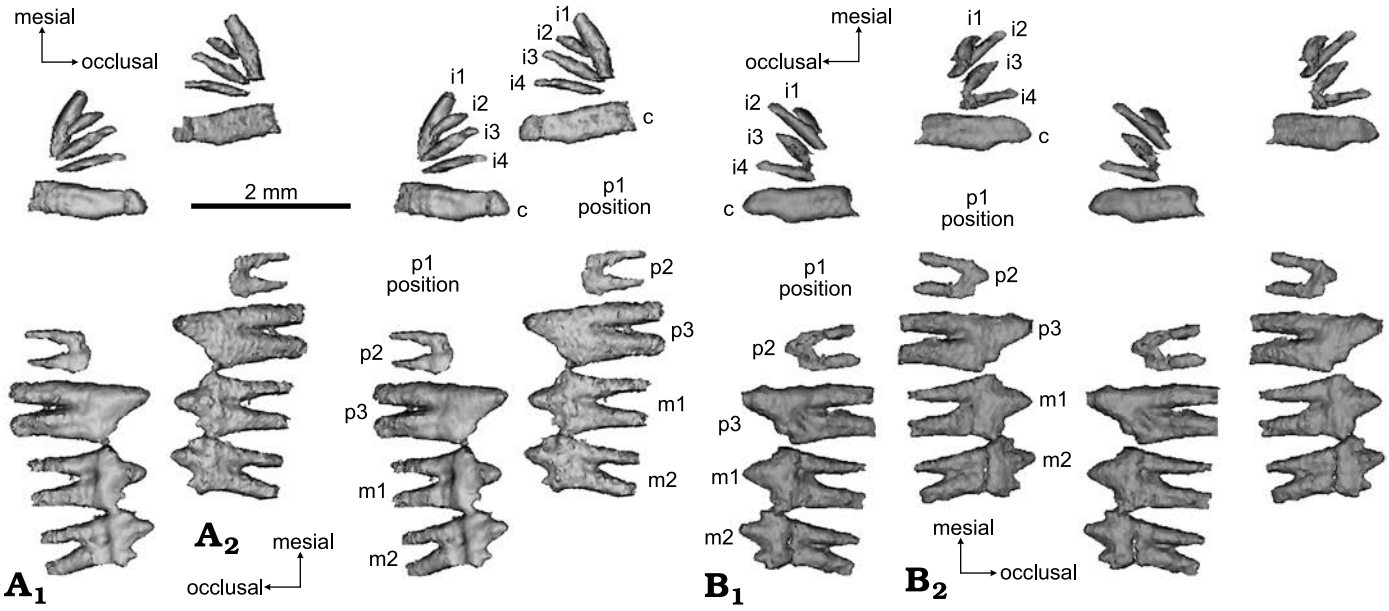

Fig. 8. CT rendering of mammaliaform *Hadrocodium wui* Luo, Crompton, and Sun, 2001 (holotype, IVPP 8275) from the Lower Lufeng Formation, Lower Jurassic of Yunnan, China. **A**. Left lower teeth (as preserved and virtually extracted from mandible): incisors, canine, incomplete premolars molars in labial (A_1, stereopairs) and lingual (A_2, stereopairs) views. The first premolar (p1) was shed and the vestige of its former alveoli recognizable on right mandible; penultimate premolar (p2) crown broken; ultimate p3 intact. **B**. Right lower teeth extracted by CT visualization, in labial (B_1, stereopairs) and lingual (B_2, stereopairs) views.

Thus the size reduction of the ultimate molar crowns (M2/m2), and the confluence and fusion of the roots of M2/m2, as seen in *H. wui* are similar to the ultimate molars of *Morganucodon watsoni* (Parrington 1971; Kermack et al. 1981; Gill 2004; Jäger et al. 2019). *Kuehneotherium praecursoris* is also interpreted to have very small ultimate upper and lower molars (Gill 2004). The comparative morphology across mammaliaforms is a strong indication that the small upper M2 with fused roots in *H. wui* type specimen is the terminal tooth in the entire dentition.

Lower incisors and canine: The left incisors are well preserved and are the basis for this description. Of the four lower incisors, i1 is twice the thickness of other incisors. The elongate i1 root extends posteriorly and medial to the roots of i2 through i4. Although the apical end of the long i1 root is not preserved (as far as can be assessed by CT), the alveolar canal of this root reaches posteriorly to a point medial to the i4 root. The i2, i3, and i4 are peg-like, and they form a size gradient with i2 being the shortest and i4 being the tallest.

The lower canine is mediolaterally compressed and the lateral profile of its crown has a lanceolate outline; the crown is slightly asymmetrical with the anterior crest being more convex and the posterior crest more concave. The canine has mediolaterally compressed roots, which are incipiently divided, with a shallow groove on the medial aspect along the root length, and a figure 8 shape in horizontal cross-section. Internally the canine roots have two divided root canals, as visualized in CT slices. The canine roots are long and penetrate the entire depth of the mandible. The lower canine of *H. wui* shows similarity to lower canines of docodontans in having incipiently divided roots with side grooves (Meng et al. 2015; Schultz et al. 2019; Panciroli et al. 2019). It is almost identical to the isolated lower canines of *Kuehneotherium praecursoris* identified from the Lower Jurassic fissure-fill deposits of the UK (Gill 2004: fig. 3.16), and bears some resemblance to the lower canines of *Morganucodon watsoni* (Mills 1971; Parrington 1971). But the root structure and crown shape differ from the more conical crown and single-rooted canine (with singular root canal) of *Morganucodon oehleri* Rigney, 1963 (BMNH2858) (Luo et al. 1995) and of *Sinoconodon rigneyi* (Fig. 9).

Lower premolars: There is a long postcanine diastema posterior to the canine and anterior to p2 in both mandibles. On the right mandible, there are two partially plugged alveoli, indicating that a two-rooted premolar was shed (Figs. 4, 6, 8). Although this anterior premolar is no longer present, its position is marked by a vestige of its alveoli. We designated this as p1 position, and we propose that the first premolar position, despite that the tooth is already lost, should be included in the tooth count and the dental formula. The comparison of the postcanine diastema will be further detailed below (see Discussion section).

The lower p2 crown, as preserved on right p2, shows a triangular outline in lateral view with a central cusp a and a posterior cusp c. The p2 is separated anteriorly by an interdental gap from the plugged p1 alveoli, also posteriorly separated by an interdental gap from p3. The tooth has two roots. The lower p3 is the tallest and most trenchant tooth of all lower teeth. Its crown is triangular in lateral outline. Its main cusp is asymmetrical in tilting anteriorly with a nearly vertical anterior crest that is shorter than the slanting posterior crest. The posterior crest bears a small cuspule, separated from the distal cingulid cuspule. The distal end of the p3 crown shows no interlocking with m1.

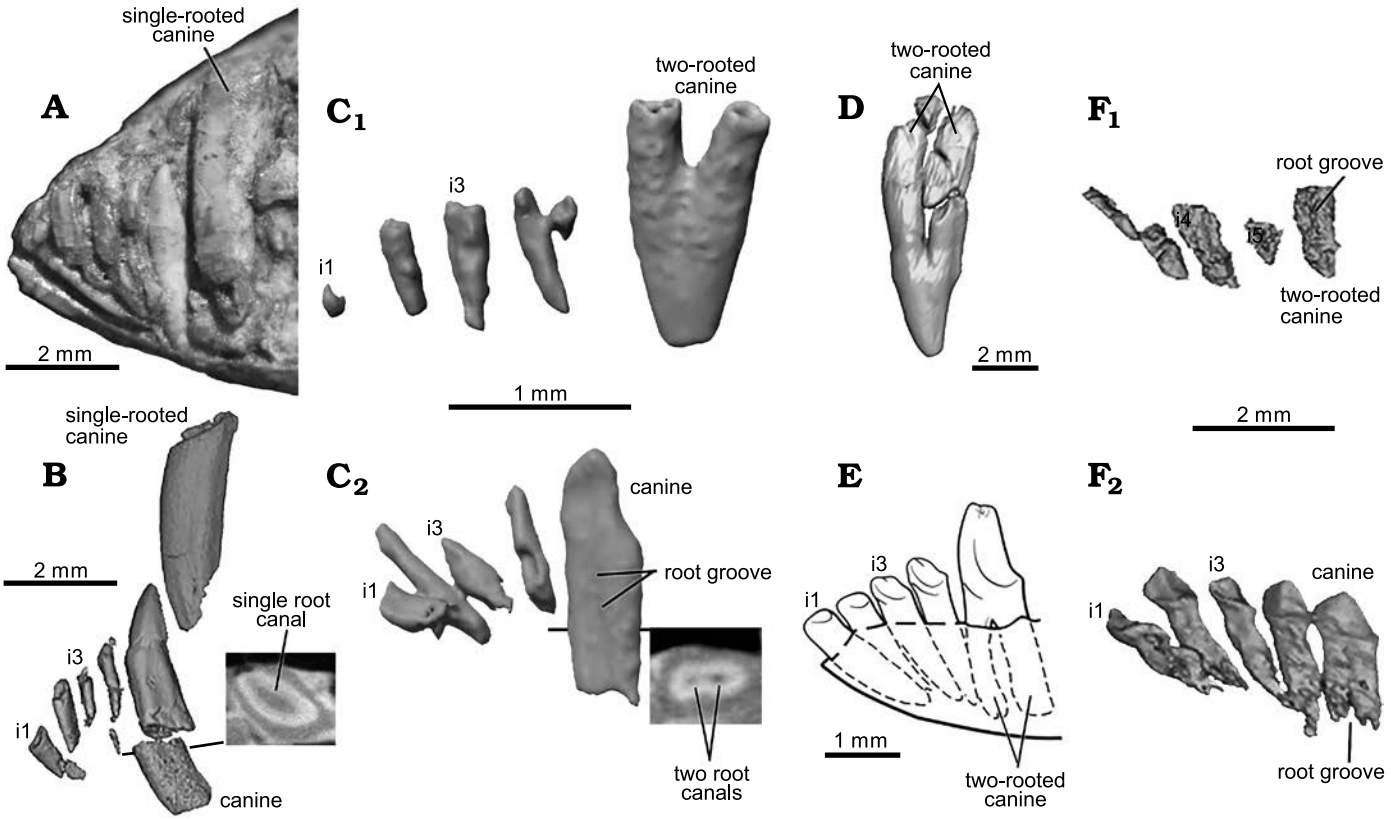

Fig. 9. Comparative morphology of incisors and canine among mammaliaforms. **A**, **B**. The morganucodontan *Morganucodon oehleri* Rigney, 1963, from the Lower Lufeng Formation, Lower Jurassic of China. **A**. CUP-FMNH 2320, type specimen. **B**. BMNH 2858, whole tooth and oblique-horizontal slice to visualize the single root canal. **C**. The mammaliaform *Hadrocodium wui* Luo, Crompton, and Sun, 2001 (holotype, IVPP 8275) from the Lower Lufeng Formation, Lower Jurassic of Yunnan, China; C_1, upper incisors and canine; C_2, lower incisors and canine. **D**. The docodontan *Haldanodon exspectatus* Kühne and Krusat, 1972 (Gui-Mam 41/75) from the Guimarota Coal Mine, Upper Jurassic of Portugal (Ruf et al. 2013; Huttenlocker et al. 2018). **E**. The docodontan *Docofossor brachydactylus* Luo, Meng, Ji, Liu, Zhang, and Neander, 2015b (BMNH 131735) from the Tiaojishan Formation, Upper Jurassic of China (Luo et al. 2015b). **F**. The docodontan *Agilodocodon scansorius* Meng, Ji, Zhang, Liu, Grossnickle, and Luo, 2015 (BMNH 00138) from the Tiaojishan Formation, Upper Jurassic of China (Meng et al. 2015b); F_1, left upper incisors and canine in lingual view; F_2, left lower incisors and canine (flipped). *Hadrocodium wui* is similar to *Haldanodon exspectatus* and *Docofossor brachydactylus* in the upper canine with fully divided roots, and to all docodonts in bilaterally compressed lower canine with partially divided (grooved) root(s) and the separated root canals inside the root(s). *Hadrocodium wui* is also similar to *Kuehneotherium praecursoris* is also similar to *Kuehneotherium* in this feature (Gill 2004). *Hadrocodium wui* differs from *Morganucodon oehleri* and *Sinoconodon rigneyi* both of which are characterized by single-rooted and tubular upper and lower canines.

Overall, the ultimate premolar of *H. wui* more closely resembles the posterior premolar type of *Kuehneotherium praecursoris* (Gill 2004; Gill et al. 2014) rather than *Morganucodon watsoni* (Kermack et al. 1973). The largest premolar (p3) of IVPP8275 is nearly identical to premolars that were interpreted to be the posterior premolars of *Kuehneotherium praecursoris* by Gill (Gill 2004: figs. 3–18; Gill et al. 2014) and by Kermack and co-workers (Kermack et al. 1968: text-fig. 3).

Lower molars: Lower m1 has a tall cusp a, and a much shorter cusp b on the mesial end of the tooth but no anterior cingulid cusp e. The posterior main cusp c is also a short cusp, separated from a distinctive distal cusp d. Cusps a–d are aligned in a straight line. The base of the crown shows no cingulid line and lacks cusps on either the labial or lingual side of the tooth.

The lower m2 has a tall cusp a and two well-developed cusps b and c. Both cusps b and c are distinctive in rising higher from the base, and different from their counterparts on m1. The main cusps a–c of m2 are aligned in a straight line similar to the straight-line cusp pattern of m1. Cusp b is closely twinned with a small (although discernible) anterolingual cuspule e. The posterior main cusp c is lower than the anterior cusp b, and c is more divergent posteriorly from the primary cusp a, such that cusp a and cusp c are farther apart from each other than cusp a and cusp b. The distal cusp d is recognizable but not well developed. The crown shows no lingual or labial cingulid structure, unlike the ultimate molars of species of *Morganucodon* that show a distinct cingulid line in m4 of *M. oehleri* and distinctive lingual cingulid plus strong cingulid cusps (such as cusp g) (sensu Mills 1971; Kermack et al. 1973; Crompton 1974; Butler 1988; Fig. 10). The lower m2 has much more confluence of its two roots than m1. *Hadrocodium wui* has a molar interlocking mechanism between the distal cusp d of m1 and the flat surface between cusp b and the very small cingulid cuspule e of m2. But there is not tooth-to-tooth interlock between p3 and m1.

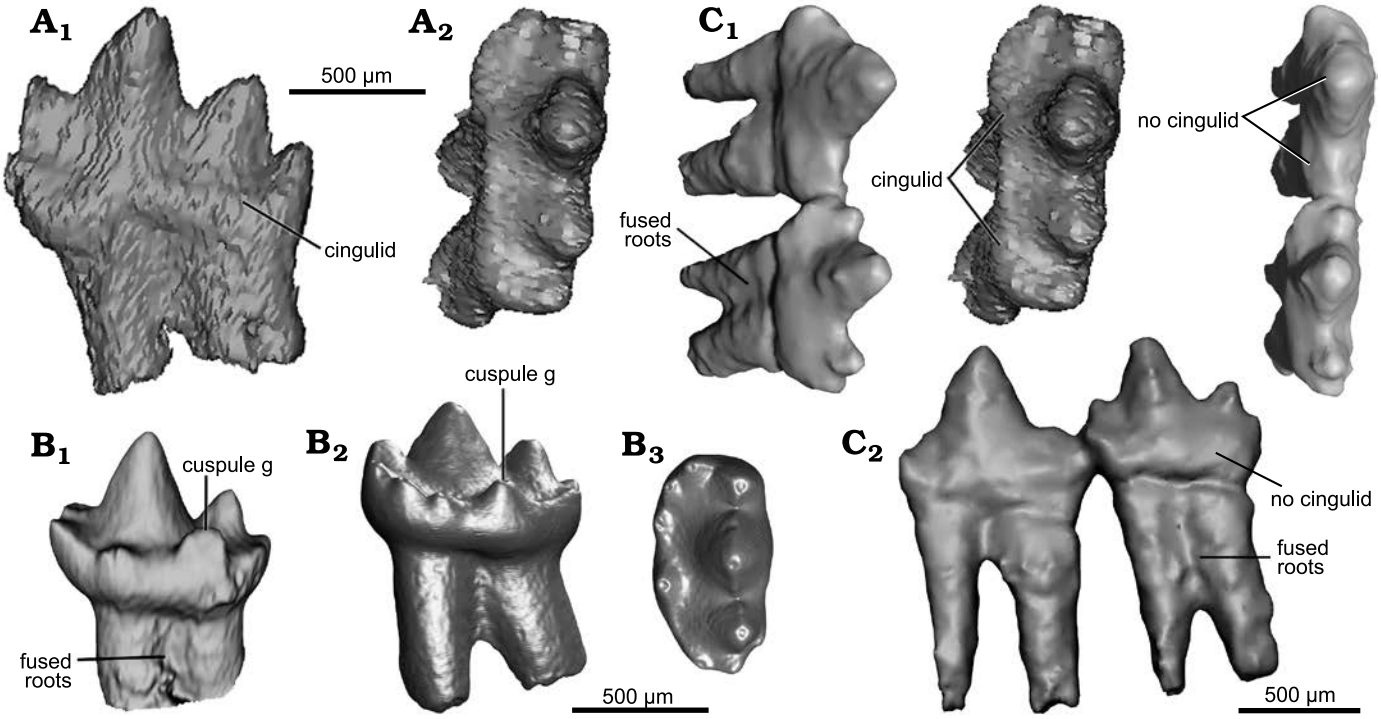

Fig. 10. Comparative morphology of lower molars of *Hadrocodium* and *Morganucodon*. **A**. The morganucodontan *Morganucodon oehleri* Rigney, 1963, from the Lower Lufeng Formation, Lower Jurassic of China. BMNH 2858, ultimate lower molar (right m4) lingual (A_1) and oblique occlusal (A_2, stereopairs) views. **B**. The morganucodontan *Morganucodon watsoni* Kühne, 1949, from the Lower Jurassic fissure fills of Wales. UMZC Eo.CR1, ultimate molar (m4); lingual view (B_1) (Jäger et al. 2019, image courtesy of Kai Jäger), lingual (B_2) and occlusal (B_3) views (Gill et al. 2014, images courtesy of Pamela Gill). **C**. The mammaliaform *Hadrocodium wui* Luo, Crompton, and Sun, 2001, from the Lower Lufeng Formation, Lower Jurassic of Yunnan, China. Holotype, IVPP 8275, right m1 and m2 in occlusal (C_1, stereopairs) and lingual (C_2) views.

The lower m2 is the smallest tooth of the p3–m1–m2 series. The left m2 is smaller than the left m1, and about 84% of the latter in length. The left m2 is also smaller than the left p3, and about 93% of the latter in length. The lower p3–m2 constitute a gradient in decreasing crown height in the successively more posterior teeth. There is a greater degree of fusion of roots in the most posterior molar as compared to the preceding postcanines.

The posteriorly decreasing size gradient of the posterior lower molars, as seen here in *H. wui*, has long been recognized for *M. watsoni* and *M. oehleri* (Parrington 1971; Kermack et al 1973, 1981; Crompton and Luo 1993; Jäger et al. 2019). This plesiomorphic pattern is also typical of docodontans, many of which are now known by complete lower molar series (Krusat 1980; Ji et al. 2006; Luo and Martin 2007; Averianov et al. 2010; Meng et al. 2015; Rougier et al. 2015; Schultz et al. 2019; Panciroli et al 2019; Zhou et al. 2019). A similar gradient in posterior decrease of molar size has been interpreted for *Kuehneotherium praecursoris* (Gill 2004), and has also been documented for *Haramiyavia* (Jenkins et al 1997; Luo et al. 2015a). Therefore, we interpret that the posteriorly decreasing gradient of lower molars is a plesiomorphic feature of perhaps all mammaliaforms of Late Triassic to Early Jurassic age, including *Hadrocodium*. The eruption of the posterior-most molar, the m2 in the case of *H. wui*, which is also the smallest of the postcanine size gradient, indicates the end of tooth development.

The two roots of the lower m2 in *H. wui* are fused along most of their length (Figs. 8, 10); the roots are fused by more than two-thirds of the root length in right m2 (Figs. 8, 10), or by half of the root length in left m2. This is structurally comparable to the terminal lower molar (m4) in morganucodontans with roots fused either partially (as in *M. oehleri*), or entirely (as in some m4s of *M. watsoni*) (Fig. 10). These fused roots of the m4 of *Morganucodon* correspond to a singular alveolus, instead of two alveoli as in preceding molars (Fig. 11; see Parrington 1971; Kermack et al. 1973).

The pattern of the smallest ultimate molar (m4) with partially or entirely fused roots is now documented in many specimens of *M. watsoni* (Parrington 1971; Kermack et al. 1973; Jäger et al. 2019). The same pattern is also present in the full-grown adult specimens of the docodontan *Borealestes serendipitus*, in which the last two lower molars show tightly compressed and partially fused roots (Panciroli et al. 2019). Here we also corroborate this pattern in an unerupted m4 of *M. oehleri* (Fig. 10). Although complete lower jaws with intact teeth are not available for kuehneotheriids, the best available postcanine reconstruction for this group (Gill 2004) suggests similarly that the last molars have tightly compressed or fused roots in *Kuehneotherium praecursoris* (Kermack et al. 1968; Gill 2004). A similar pattern also occurs in *Kuehneotherium stanislavi* Debuysschere, 2017 (Debuysschere 2017). Based on this comparison, we interpret that the lower m2 of the *H. wui* type specimen, with its fused roots, is the last and

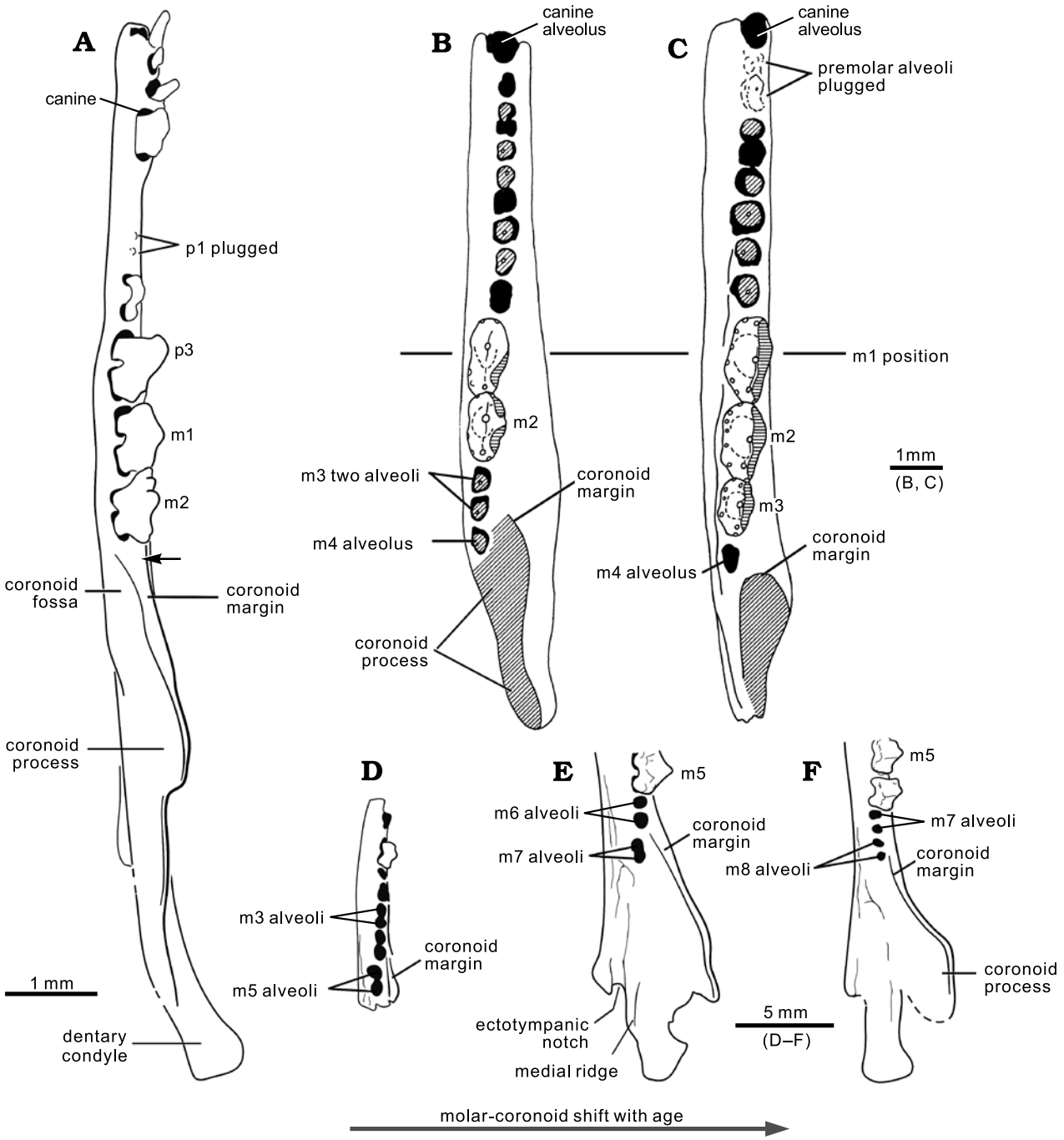

Fig. 11. Comparison of the mandible of *Hadrocodium* with the mandibular growth stages of *Morganucodon* and *Docodon*. **A**. The mammaliaform *Hadrocodium wui* Luo, Crompton, and Sun, 2001 (holotype, IVPP 8275) from the Lower Lufeng Formation, Lower Jurassic of Yunnan, China (arrow indicates the retro-molar space and feature of adult). **B**, **C**. Mandibular growth stages of the morganucodontan *Morganucodon watsoni* Kühne, 1949 (= "*Eozostrodon parvus*") from the Lower Jurassic fissure fills of Wales (Parrington 1971); adult (**B**) and the oldest-known adult (**C**) (respectively specimens D60 and D120 in Parrington 1971: fig. 3). **D**–**F**. Mandibular growth stages of the docodontan *Docodon victor* Schultz, Bhullar, and Luo, 2019, from the Morrison Formation, Upper Jurassic of Wyoming, USA. **D**. YPM 23748, juvenile. **E**. YPM 11823, adult. **F**. YPM 11826, the oldest-known adult. In *H. wui*, the ultimate molar is positioned in front of the coronoid process base. This is an adult feature well documented in the successively older (or the oldest-known) adult individuals in the growth series of other mammaliaforms. *Morganucodon watsoni* shows such a growth pattern: a positional shift of the ultimate molar (m4) anteriorly to the base of coronoid process in successively older individuals; the ultimate molar has a single alveolus for its fused or confluent root(s) in most cases (Parrington 1971; Pamela Gill, personal communication 2021). *Docodon victor* shows a similar growth pattern of a shift of the coronoid process relative to the last molar(s) of the toothrow. The youngest-available individual *D. victor* (YMP23748) shows the last molar (m5) is medial to the coronoid process. In the adult (YPM11823) the last molar (m7) is shifted more anteriorly. In the oldest-available individual (YPM11826), the ultimate molar (m8) is shifted to the anterior, as the coronoid process is shifted posteriorly relative to the toothrow (Schultz et al. 2019). The placement of the ultimate molar with a retro-molar space anterior to the base of the coronoid in the oldest-available adult specimen of *D. victor* is similar to that of *H. wui*. D–F, stylistic illustrations based on CT visualizations by Schultz et al. (2019).

terminal molar to erupt, and equivalent to the terminal molar (m4) of species of *Morganucodon* (Fig. 8) and last molars (m5 and m6) of *B. serendipitus* (Panciroli et al. 2019).

Molar occlusion: The upper and lower molars, now visualized from CT scans (Figs. 6–8), show several features previously hidden by occlusal association of upper and lower teeth. This is helpful to rectify several incorrect interpretations of molar occlusion in our earlier study (Luo et al. 2001: fig. 1). The new pattern of correspondence between cusps of upper and lower molars is different by half of a cusp from the previous incorrect reconstruction (Luo et al. 2001: fig. 1).

The upper postcanines show more of a lingual inclination than the more vertically oriented lower molars. The upper molar lingual inclination is common for the triconodont-like dentition of other mammaliaforms, such as *Morganucodon*, and of eutriconodontans (Jäger et al. 2019, 2020, 2021). This pattern is obvious from the better preserved right side of the skull, which shows more lingually inclined upper teeth in CT sections (Figs. 4, 5).

The lower m1 cusp a is aligned with the embrasure between the upper P3 and M1 (Fig. 6). The anterolabial surface of the large cusp a of m1 occludes with the postero-lingual aspect of the cusp A of the upper P3. Because the cusp b on m1 is relatively low, the entire anterolabial aspect of m1 likely forms a continuous contact facet to P3. The posterolabial aspect of cusp a of m1 occludes with the anterolingual surface of upper M1 across both cusp A and cusp B. As cusp c of the m1 is relatively small (better preserved on the left m1), the m1 crown forms a continuous wear surface between cusps a and c. It also appears that m1 is more strongly worn than m2, and this is consistent with the greater degree of wear of m1 as the first erupted molar of the molar row, as in other mammaliaforms with diphyodont tooth replacement. The lower m2 primary cusp a occludes into the embrasure between the posterior cusp C of M1 and the anterior cusp B of M2, while m1 cusp b can contact the lingual surface of cusp C of the upper M1 (Fig. 6).

The upper M1 primary cusp A occludes into the embrasure between the cusp c of lower m1 and cusp b of m2. The lingual surface of cusp C of the M1 has a discernible facet that matches the labial facet across cusps a and b of the lower m2.

A striking pattern of the molar occlusion is the unique occlusal match of M1–M2 vs. m2 as a consequence of size disparity of the very small upper M2 vs. larger lower m2. Because of the much reduced size of the upper M2 relative to m2, cusp A of the M2 directly corresponds to the shallow notch between cusp a and cusp c of m2. On the labial side of the lower m2, there are wear facets on the shallow valley. Overall the lower p3–m1–m2 occlude in the embrasure of the upper P3–M1–M2, but due to the size difference of M2, the M2 cusp A occludes between cusps a and c of the lower m2.

In extant mammals, wear facets developed in the ultimate molars would indicate the terminal stage of dental ontogeny (Anders et al. 2011), as the ultimate molars are the last to erupt in the full permanent dentition in extant marsupials (van Nievelt and Smith 2005a; Astua and Leiner 2008) and placentals (Smith 2000; Anders et al. 2011). Thus, the presence of a wear pattern on M2/m2 suggests that the *H. wui* holotype specimen is an adult, or approaching the adult stage (see Discussion for further details on growth stage assessment).

Stratigraphic and geographic range.—Upper Red Beds of Lower Lufeng Fromation, Yunnan, China; Dadi Locality in Lufeng Basin.

Discussion

For the mammaliaforms of the Late Triassic and Early Jurassic, *Hadrocodium wui* is very small (rostro-condylar length of the skull equals 12 mm), about 40% the length of the smallest-known specimen of *Morganucodon oehleri* (Luo et al. 2004). In our redescription, we provide additional support for an adult ontogenetic age of the type specimen despite its small size (Crompton and Luo 1993; Luo et al. 2001). Using several dental and mandibular features that are known to change with developmental stages in other mammaliaforms, we polarize the variation of these characters along a continuum of juvenile-adult growth, for a comparative assessment of the growth stage as a proxy to the age estimate of *H. wui*.

Absence of un-erupted replacement teeth.—There is no un-erupted replacement tooth in any of the incisor, canine, or premolar loci of *H. wui*. In extant shrew species, which are some of the smallest placental mammals, the incisors and canines have typical diphyodont (two-generational) replacements. Neonatal or juvenile individuals frequently have an un-erupted replacement tooth below the deciduous teeth, or the erupting replacement teeth are juxtaposed with the deciduous teeth (Ziegler 1971, 1972). In some shrews, the primary generation of deciduous teeth is developed embryonically, but these teeth are resorbed before eruption. Only the secondary generation of (permanent) incisors or canine erupts (Kindahl 1959; Bloch et al. 1998). In a more recent study on tooth development in the shrew *Sorex araneus*, it was demonstrated that only the last premolar locus develops both the deciduous and the permanent replacement tooth (Järvinen et al. 2008).

By comparison to these small extant placentals, the absence of un-erupted replacement teeth in any incisor or canine loci in *H. wui* suggests one of two developmental scenarios: (i) the *H. wui* specimen had grown beyond the juvenile stages of replacing incisors and canines, or (ii) it was similar to adults of those small placentals in which the deciduous predecessors of diphyodont loci were present as embryonic tooth germs but resorbed prior to birth of the animal, and only adult permanent teeth developed to full eruption. Either scenario would suggest *H. wui* type specimen is an adult, or a young adult at a late growth stage.

M2/m2 are the terminal molar loci.—The upper M2 and lower m2 have already developed occlusal wear, as the much reduced M2 occludes with m2 (Fig. 6). The roots of the molar are extensively fused in m2 and completely fused in M2. The ultimate molars are the smallest teeth of the posteriorly decreasing gradient of m2 and more posterior molars in all stem mammaliaform clades. In *Morganucodon* species, both the upper and lower ultimate molars have stronger fusion of their roots than the more anterior molars (Fig. 8) (Parrington 1971; Jäger et al. 2019). In the docodontan *Borealestes serendipitus*, the lower ultimate molar has partially fused and tightly compressed roots (Panciroli et al. 2019). This is strong evidence that the M2/m2 are the ultimate molars because they have identical characteristics of ultimate molars of other mammaliaforms.

In extant didelphid marsupials, the end of cranio-dental growth is marked by full eruption of the ultimate upper molar (M4), which occurs after eruption of the ultimate lower molar (m4) (van Nievelt and Smith 2005a, b; Astua and Leiner 2008). By comparison, the ultimate upper M2 has erupted and is in full occlusion with the lower m2 in *H. wui*, and this occlusal function generated wear facets on the lower m2 between cusps a and c (Fig. 6). From this we infer that the dentition of the type specimen of *H. wui* was fully erupted. In extant placentals, the dental development approaches the end stage when the ultimate upper and lower molars are occluding (Anders et al. 2011) as these are the last of the adult teeth to erupt (Smith 2000). By this comparison, the skull of *H. wui* is either a fully grown adult, or at least a young adult that is dentally mature and capable of independent feeding.

Postcanine diastema.—By our conservative estimate of premolar count, the prominent diastema on the mandible shows two plugged alveoli of p1. This suggests that a two-rooted premolar had been shed. In the upper jaw, there is a single dimple in the diastema between the canine and the upper P2, indicating that an anterior upper premolar (P1) was lost and its alveolus was plugged (Figs. 6, 7). Taking into account these lost premolars, we interpret, conservatively, that *H. wui* had three upper and three lower premolar positions. A less likely alternative is that the postcanine diastema may correspond to more than one premolar, and if so *H. wui* would have had four premolar loci. However, there are no traces of tooth alveoli in the dentary anterior to p1 position and in the maxilla anterior to P1 position, thus no evidence that more than one premolar was lost in the existing diastemata. Thus we interpret that *H. wui* has only three premolars.

The timing for shedding premolars appears to differ between the left and right upper jaws. Further, the loss of both P1 and P2 on the left upper jaw suggests that the loss of premolar 2 occurred earlier on the upper jaw than on the mandibles. The developmental loss of some premolars in *H. wui* suggests that the animal already experienced tooth replacement process, which again indicates it was dentally mature, but not a juvenile, despite its small skull size.

A postcanine diastema that enlarges in successively older individuals has been well characterized for other mammaliaforms. *Sinoconodon rigneyi* has a postcanine diastema, which first appears in the youngest-known juveniles, and then enlarges with age in successively older individuals as more anterior premolars were shed without being replaced (Crompton and Luo 1993; Zhang et al. 1998). In larger (presumably older) individuals the postcanine diastema is so much enlarged that it can be as long as the length of the entire remaining postcanine row (Crompton and Luo 1993). *Morganucodon watsoni* is also known for a similar age-related development of this diastema (Fig. 11), and older individuals of *M. watsoni* can lose up to two lower premolars (Mills 1971; Parrington 1971; Kermack et al. 1973). This type of growth-related loss of up to two premolars is also documented in *Dinnetherium nezorum* (Fig. 1; see also Crompton and Luo 1993) and in *Kuehneotherium praecursoris* (Gill 1974, 2004). But this feature is absent in older individuals of *Docodon victor* and *Borealestes serendipitus* among docodontans (Schultz et al. 2019; Panciroli et al. 2019, 2021).

Non-mammaliaform cynodonts, such as diademodontids, traversodontids, and tritylodontids, are also characterized by prominent development of age-dependent postcanine diastemata (Hopson 1971; Crompton and Luo 1993), or post-incisor diastemata (Hoffman and Rowe 2018). The age-related growth of this diastema in cynodonts is similarly formed by shedding of teeth without replacement of a succeeding tooth in the same locus (Hopson 1971; Hoffman and Rowe 2018). Based on the consistent developmental pattern of the postcanine diastema in other mammaliaforms and cynodonts, the presence of a sizable tooth gap in the type specimen of *H. wui* is an indication that the individual already had significant alterations to the dental arcade related to aging.

Molar–coronoid alignment and retro-molar space.—The ultimate molar (m2) is aligned directly in front of the coronoid process, and there is a retro-molar space between m2 and the rising base of the coronoid process (Fig. 11A: arrow). These features are interpreted to be mandibular characteristics of adult individuals, by comparison to the more complete growth-related variation of the mandibles in other mammaliaforms (Fig. 11). In an earlier study of the growth variation of *Morganucodon watsoni* (= "*Eozostrodon parvus*"), Parrington (1971) recognized an age-related shift of the posterior molars relative to the coronoid process. In juveniles and early young adults, the successively more posterior molars erupt medial to the anterior margin of the coronoid process. But in the oldest individuals of this growth series, the ultimate molars have shifted anteriorly relative to the coronoid process, and the ultimate molar is in front of the coronoid process (Fig. 11B, C). However, in some rare instances, the ultimate molar remains antero-medial to the base of the coronoid process in *M. watsoni* (Pamela Gill, personal communication 2021). It is possible that these individuals have a complete dentition but have not yet completed the growth of the lower jaw.

This pattern is also present in the growth series of *Docodon victor* Schultz, Bhullar, and Luo, 2019 (Schultz et al. 2019: fig. 4). In the youngest-available individual in the growth series of *D. victor*, the last molar (m5) has just erupted medial to the coronoid process. In an adult mandible, m5 and m6 have already shifted anteriorly to the front of the coronoid, while the last molar (m7) is still medial to the coronoid. In the oldest-available individual of this growth series, the ultimate molar (m8) and penultimate m7 have both shifted anteriorly, while the coronoid process is shifted posteriorly relative to the toothrow, such that the toothrow including the last m8 is aligned with the coronoid process (Schultz et al. 2019: fig. 4). The position of the ultimate molar anterior to the base of the coronoid process in the oldest-available adult specimen of *D. victor* is similar to that of *H. wui*. By this growth-related coronoid-molar re-alignment, the *H. wui* type specimen is most likely an adult, despite its minute size.

To summarize, the above-mentioned characters indicate that the specimen of *H. wui* is at least a young adult, by the absence of any un-erupted replacement teeth. Its status as a young or fully grown adult is also supported by growth-related tooth or mandibular features that can be clearly differentiated along the juvenile-adult continuum of growth in other mammaliaforms with more complete growth stages, as seen in morganucodontans (Parrington 1971; Kermack et al. 1973, 1981; Crompton and Luo 1993; Jäger et al. 2019), *Sinoconodon* (Crompton and Luo 1993; Zhang et al. 1998), and docodontans (Schultz et al. 2019; Panciroli et al. 2019).

Taxonomic characteristics of *Hadrocodium*.—*Hadrocodium wui* can be easily distinguished from *Morganucodon oehleri* and *Sinoconodon rigneyi* from the Lower Lufeng Formation by a list of discrete characters:

(i) Upper canine of *H. wui* has fully divided roots, instead of the single root of the canine of species of *Morganucodon* and *Sinoconodon rigneyi* (Parrington 1973; Kermack et al. 1973, 1981; Zhang et al. 1998). The fully divided canine roots of *H. wui* are more similar to those of *Haldanodon* and *Docofossor* (Fig. 9) than *Morganucodon* and *Sinoconodon*.

(ii) Incipient division of the lower canine roots has two root canals, as in the canine of *Kuehneotherium praecursoris* and *Agilodocodon scansorius* Meng, Ji, Zhang, Liu, Grossnickle, and Luo, 2015, instead of single, tubular root of the lower canine of *Morganucodon* and *Sinoconodon* (Fig. 9).

(iii) Upper and lower molars of *H. wui* have no distinct cingulum or cingulid as opposed to the condition in *M. oehleri* (Fig. 10). The ultimate molar (m2) is much smaller than the ultimate molar (m4) of *M. oehleri*. Molars of *Hadrocodium* are also distinguishable from those of *Dinnetherium* in lacking the cingulid structure including cingulid cusps.

(iv) A steep decrease in size of posterior upper postcanines (P3–M1–M2) is observed in *Hadrocodium.* This is more conspicuous than the size decrease in other mammaliaforms, such as M2–M3–M4 of morganucodontans and docodontans.

(v) *Hadrocodium* has a unique combination of embrasure occlusion of M1–M2 with m1–m2, with M2 cusp A occluding between cusp b and cusp c of m2 (Fig. 6). This is an autapomorphic character of *Hadrocodium*.

Size disparity among the earliest mammaliaforms.—Mammaliaform taxa from the Late Triassic and Early Jurassic are already known from a range of body sizes, and *Hadrocodium* further expands the scope of this disparity. Although the stem mammaliaforms went through an evolutionary bottle-neck of size reduction in phylogeny as compared to non-mammaliaform cynodonts (Lautenschlager et al. 2018), this does not preclude the basalmost mammaliaforms showing size differentiation among themselves. For example, the largest specimen of *Sinoconodon rigneyi* has a skull length over 60 mm, and is estimated to have a body mass over 500 grams (Kielan-Jaworowska et al. 2004; Luo et al. 2004). Among the best sampled mammaliaforms in the Lower Jurassic fissure-fill sediments of the United Kingdom (reviewed by Parrington 1971; Kermack et al. 1973; Evans and Kermack 1994; Gill 2004; Clemens 2011), several morganucodontan taxa, such as *Bridetherium dorisae* and *Pacyodon davidi*, are now recognized by differences in cusp morphology and also by differences in tooth sizes (Clemens 2011). Elsewhere in the world, mammaliaform faunas of the Early Jurassic age display a wide generic diversity especially among docodontans and morganucodontans through the Triassic–Jurassic transition (Clemens 2011; Debuysschere et al. 2015). Parrington (1971, 1973) and Mills (1971) were the first to recognize that the posterior molars of *Morganucodon*-related taxa can be classified into different size groups, and the *Morganucodon*-like molars from fissure-fill sediments are polymorphic. Of these, some taxa of small tooth sizes have been further recognized as different taxa of morganucodontans (Clemens 2011). The posterior-most molars in these small-sized taxa (less than 1 mm in tooth length) are different from the m4s of *Morganucodon watsoni* (Clemens 2011). Mammaliaform taxa from the Late Triassic of Continental Europe have also long been known to show different tooth morphology and size disparity (Clemens 1980; Sigogneau-Russell and Hahn 1994; Debuysschere et al. 2015; Debuysschere 2017). Implicit in the discussion of size disparity and distinctive morphological differences is that the tooth size can differentiate these mammaliaform taxa if corroborated by morphological differences. Importantly, the small size of a fossil does not necessarily mean it would be a juvenile individual of a larger species (Clemens 2011; Debuysschere et al. 2015).

Hadrocodium wui adds to the size disparity of the Early Jurassic Lufeng mammaliaforms. The Lower Lufeng Formation mammaliaform assemblage has three distinctive size groups: *Sinoconodon rigneyi* is the largest (skull size ranges from the smallest at 22 mm in length to the largest at 62 mm in length); *Morganucodon oehleri* is intermediate in body size (skull size ranges from the smallest at 27 mm in length up to the largest around 38 mm in length) (Luo et

al. 2004); *H. wui* at 12 mm in skull length is the smallest (Luo et al. 2001). The size difference between these taxa is now also corroborated by differences of *Hadrocodium* from other mammaliaforms in postcanine formula, canine structure, and occlusion of molar crowns. The posterior molars may also show variable root structure.

Implications for middle ear evolution of mammals.—This new CT study has revealed that the middle ear elements were still attached to the postdentary trough in *H. wui*. Given that *Hadrocodium* is close to the ancestral node of the crown Mammalia, this adds to the evidence that stem mammaliaforms all had middle ear elements connected to the mandible (Luo et al. 2016, 2017; Luo and Manley 2020). The detached middle ear evolved separately in monotremes, multituberculates, and crown therians.

Conclusions

The CT scans and visualization show that *Hadrocodium wui* has plesiomorphic mandibular and middle ear characters. The new dental characters of *H. wui* indicate that it differs from *Morganucodon oehleri* and *Sinoconodon rigneyi* from the same fauna of the Lower Jurassic Lower Lufeng Formation. Additionally, the newly characterized features of the holotype of *H. wui* suggest that it is an adult, or a young adult, capable of independent feeding. It is not a juvenile of an existing mammaliaform taxon of the same fauna.

Acknowledgements

For the many contributions by our esteemed colleague Professor Richard L. Cifelli (Oklahoma Museum of Natural History, Norman, USA) to the study of early mammalian evolution and his extensive field exploration of Mesozoic mammal fossils, it is our privilege to be able to contribute this new study on a Jurassic mammaliaform for the festschrift issue of *Acta Palaeontologica Polonica* in his honor. We are grateful for the invitation by Brian M. Davis (University of Louisville, USA). This study would not be possible without the discovery the fossil of *Hadrocodium* by Xiaochun Wu (Canadian Museum of Nature, Ottawa, Canada), and we are much indebted to Ai-Lin Sun (IVPP) and Xiaochun Wu for making this precious specimen available for our studies. The studies of *Hadrocodium* would have been impossible without the supreme skills of the late William A. Amaral (MCZ) who patiently prepared out the external morphologies of this very small fossil. We like to thank Richard Ketcham (Jackson School of Geosciences, University of Texas, Austin, USA) for scanning the fossil, and Thomas E. Macrini (University of Texas, Austin, USA and St. Mary's University, San Antonio, USA) for helping to process the CT data. We also thank Qing-Jin Meng and Jianjun Li (both BMNH), for allowing us to access comparative specimens during this study, and Pamela Gill (University of Bristol, UK) and Kai R.K. Jäger (University of Bonn, Germany) for providing images of *Morganucodon* teeth for our study. During the course of this work, we benefitted from discussion with Richard L. Cifelli, James A. Hopson (The University of Chicago, USA), Thomas Martin (University of Bonn, Germany), Yuan-Qing Wang (IVPP), Xiao-Chun Wu, Kai R.K. Jäger and the late Professor William A. Clemens. For interpretation of mammaliaform mandibles and teeth, we benefited from the extensive feedback and comment by Pamela Gill, Stephan Lautenschlager (University of Birmingham, UK), Elsa Panciroli (University of Oxford, UK), and Julia A. Schultz (University of Bonn, Germany). The authors are very grateful for the thoughtful critiques and many suggestions for improvement by Brian Davis, Pamela Gill, and Thomas Martin, although any errors or insufficiency remain the authors' own.

References

Anders, U., Koenigswald, W. v, Ruf, I., and Smith, B.H. 2011. Generalized individual dental age stages for fossil and extant placental mammals. *Paläontologische Zeitschrift* 85: 321–339.

Astua, D. and Leiner, N.O. 2008. Tooth eruption sequence and replacement pattern in woolly opossums, genus *Caluromys* (Didelphimorphia: Didelphidae). *Journal of Mammalogy* 89: 244–251.

Averianov AO, Lopatin AV, Krasnolutskii SA, Ivantson SV. 2010. New docodontans from the Middle Jurassic of Siberia and reanalysis of Docodonta interrelationships. *Proceedings of the Zoological Institute of Russian Academy of Sciences* 314: 121–148.

Bi, S.-D., Wang, Y.-Q., Guan, J., Sheng, X., and Meng, J. 2014. Three new Jurassic euharamiyidan species reinforce early divergence of mammals. *Nature* 514: 579–584.

Bloch, J.I., Rose, K.D., and Gingerich, P.D. 1998. New species of *Batodonoides* (Lipotyphla, Geolabididae) from early Eocene of Wyoming: smallest known mammal? *Journal of Mammalogy* 79: 804–827.

Butler, P.M. 1988. Docodont molars as tribosphenic analogues (Mammalia, Jurassic). *In*: D.E. Russell, J.-P. Santoro, and D. Sigogneau-Russell (eds.), Teeth Revisited: Proceedings of the VIIth International Symposium on Dental Morphology. *Mémoirs du Muséum national d'Histoire naturelle* C 53: 329–340.

Clemens, W.A. 1980. Rhaeto-Liassic mammals from Switzerland and West Germany. *Zitteliana, Abhandlungen der Bayerischen Staatssammlung für Paläontologie und Historische Geologie* 5: 51–92.

Clemens, W.A. 2011. New morganucodontans from an Early Jurassic fissure filling in Wales (United Kingdom). *Palaeontology* 54: 1139–1156.

Crompton, A.W. 1974. The dentition and relationships of the southern African Triassic mammals, *Erythrotherium parringtoni* and *Megazostrodon rudnerae*. *Bulletin of the British Museum (Natural History), Geology* 24: 397–437.

Crompton, A.W. and Jenkins, F.A., Jr. 1968. Molar occlusion in Late Triassic mammals. *Biological Reviews* 43: 427–458.

Crompton, A.W. and Luo, Z.-X. 1993. The relationships of the Liassic mammals *Sinoconodon*, *Morganucodon oehleri* and *Dinnetherium*. *In*: F.S. Szalay, M.J. Novacek, and M.C. McKenna (eds.), *Mammal Phylogeny. Volume 1*, 30–44, Springer-Verlag, New York.

Crompton, A.W. and Sun, A.-L. 1985. Cranial structure and relationships of the Liassic mammal *Sinoconodon*. *Zoological Journal of Linnean Society* 85: 99–119.

Davis, B.M. 2012. Micro-computed tomography reveals a diversity of peramuran mammals from the Purbeck Group (Berriasian) of England. *Palaeontology* 55: 789–817.

Debuysschere, M. 2017. The Kuehneotheriidae (Mammaliaformes) from Saint-Nicolas-de-Port (Upper Triassic, France): a systematic review. *Journal of Mammalian Evolution* 24: 127–146.

Debuysschere, M., Gheerbrant, E., and Allain, R. 2015. Earliest known European mammals: a review of the Morganucodonta from Saint-Nicolas-de-Port (Upper Triassic, France). *Journal of Systematic Palaeontology* 13: 825–855.

Evans, S.E. and Kermack, K.A.1994. Assemblages of small tetrapods from the Early Jurassic of Britain. *In*: N.C. Fraser and H.-D. Sues (eds.), *In the Shadow of the Dinosaurs, Early Mesozoic Tetrapods*, 271–283. Cambridge University Press, Cambridge.

Gao, C.-L., G. P. Wilson, Z.-X. Luo, A.M. Maga, Q.-J. Meng, and Wang,

X.-R. 2009. A new mammal skull from the Lower Cretaceous of China with implications for the evolution of obtuse angled molars and "amphilestid" eutriconodonts. *Proceedings of Royal Society (London) Series B* (Biological Sciences) 277: 237–246.

Gebo, D.L. Dagosto, M., Beard, K.C., and Tao, Q. 2000. The smallest primate. *Journal of Human Evolution* 38: 585–594.

Gill, P.G. 1974. Resorption of premolars in the early mammal *Kuehneotherium praecursoris. Archives of Oral Biology* 19: 327–328.

Gill, P.G. 2004. Kuehneotherium *From the Mesozoic Fissure Fillings of South Wales*. 286 pp. Ph.D. Dissertation, University of Bristol, Bristol.

Gill, P.G., Purnell, M.A., Crumpton, N., Robson Brown, K., Gostling, N.J., Stampanoni, M., and Rayfield, E.J. 2014. Dietary specializations and diversity in feeding ecology of the earliest stem mammals. *Nature* 512: 303–306.

Hoffman, E.A. and Rowe, T.B. 2018. Jurassic stem-mammal perinates and the origin of mammalian reproduction and growth. *Nature* 561: 104–108.

Hopson, J.A. 1971. Postcanine replacement in the gomphodont cynodont *Diademodon*. *In*: D.M. Kermack and K.A. Kermack (eds.), *Early Mammals*, 199–216. Academic Press, London.

Huttenlocker, A.K., Grossnickle, D.M., Kirkland, J.I., Schultz, J.A., and Luo, Z.-X. 2018. Late-surviving stem mammal links the lowermost Cretaceous of North America and Gondwana. *Nature* 558: 109–112.

Järvinen, E., Välimäki, K., Pummila, M., Thesleff, I., and Jernvall, J. 2008. The taming of the shrew milk teeth. *Evolution & Development* 10: 477–486.

Jäger, K.R.K., Cifelli, R.L., and Martin, T. 2020. Molar occlusion and jaw roll in early crown mammals. *Scientific Reports* 10: 22378.

Jäger, K.R.K., Cifelli, R.L., and Martin, T. 2021. Tooth eruption in the Early Cretaceous British mammal *Triconodon* and description of a new species. *Papers in Palaeontology* 7: 1065–1080, published online in 2020.

Jäger, K.R.K., Gill, P.G., Corfe, I.J., and Martin, T. 2019. 3D Occlusion and dental function of *Morganucodon* and *Megazostrodon*. *Journal of Vertebrate Paleontology* 39 (3): e1635135.

Jenkins, F.A., Jr., Crompton, A.W., and Downs, W.R. 1983. Mesozoic mammals from Arizona: new evidence on mammalian evolution. *Science* 222: 1233–1235.

Jenkins, F.A., Jr., Gatesy, S.M., Shubin, N.H., and Amaral, W.A. 1997. Haramiyids and Triassic mammalian evolution. *Nature* 385: 715–718.

Ji, Q., Luo, Z.-X., Yuan ,C.-X., and Tabrum, A.R. 2006. A swimming mammaliaform from the Middle Jurassic and ecomorphological diversification of early mammals. *Science* 311: 1123–1127.

Jürgens, K.D. 2002. Estrucan shrew muscle: the consequence of being small. *The Journal of Experimental Biology* 205: 2161–2166.

Kermack, D.M., Kermack, K.A., and Mussett, F. 1968. The Welsh pantothere *Kuehneotherium praecursoris*. *Journal of the Linnean Society (Zoology)* 47: 407–423.

Kermack, K.A. and Mussett, F. 1958. The jaw articulation of the Docodonta and the classification of Mesozoic mammals. *Proceedings of the Royal Society, London* 149: 204–215.

Kermack, K.A., Mussett, F., and Rigney, H.W. 1973. The lower jaw of *Morganucodon*. *Zoological Journal of Linnean Society* 53: 87–175.

Kermack, K.A., Mussett, F., and Rigney, H.W. 1981. The skull of *Morganucodon*. *Zoological Journal of Linnean Society* 71: 1–158.

Kielan-Jaworowska, Z., Cifelli, R.L., and Luo, Z.-X. 2004. *Mammals from the Age of Dinosaurs: Origins, Evolution, and Structure*. xv + 630 pp. Columbia University Press, New York.

Kindahl, M. 1959. Some aspects of the tooth development in soricidae. *Acta Odontologica Scandinavica* 17: 203–237.

Krusat, G. 1980. Contribução para o conhecimento da fauna do Kimeridgiano da mina de lignito Guimarota (Leiria, Portugal). IV Parte. *Haldanodon exspectatus* Kuhne & Krusat 1972 (Mammalia, Docodonta). *Memórias dos Serviços Geológicos de Portugal* 27: 1–79.

Kühne, W.G. 1949. On a triconodont tooth of a new pattern from a fissure-filling in South Glamorgan. *Proceedings of the Zoological Society of London* 119: 345–350.

Kühne, W.G. and Krusat, G. 1972. Legaliesierung des taxon *Haldanodon* (Mammalia, Docodonta). *Neues Jahrbuch für Geologie, Paläontologie und Mineralogie, Monatshefte* 5: 300–302.

Laaß, M. and Kaestner, A. 2017. Evidence for convergent evolution of a neocortex-like structure in a late Permian therapsid. *Journal of Morphology* 278:1033–1057.

Lautenschlager, S., Gill, P.G., Luo, Z.-X., Fagan, M.J., and Rayfield, E.J. 2017. Morphological evolution of the mammalian jaw adductor complex. *Biological Reviews* 92: 1910–1940.

Lautenschlager, S., Gill, P.G., Luo, Z.-X., Fagan, M.J., and Rayfield, E.J. 2018. The role of miniaturisation in the evolution of the mammalian jaw. *Nature* 561: 533–537.

Liu, L., Zhang, J., Rheindt, F.E., Lei, F., Qu, Y., Wang, Y., Zhang, Y., Corwin, S., Nie, W., Wang, J., Yang, F., Chen, J., Edwards, S. V., Meng J., and Wu, S. 2017. Genomic evidence reveals a radiation of placental mammals uninterrupted by the KPg boundary. *Proceedings of National Academy of Sciences USA* 114: E7282–E7290.

Luo, Z.-X. 1994. Sister taxon relationships of mammals and the transformation of the diagnostic mammalian characters. *In*: N.C. Fraser and H.-D. Sues (eds.), *The Shadow of Dinosaurs: Early Mesozoic Tetrapods*, 98–128. Cambridge University Press, Cambridge.

Luo, Z.-X. 2007. Transformation and diversification in the early mammalian evolution. *Nature* 450: 1011–1019.

Luo, Z.-X. 2011. Developmental patterns in Mesozoic evolution of mammal ears. *Annual Review of Ecology, Evolution and Systematics* 42: 355–380.

Luo, Z.-X. and Manley, G.A. 2020. Origins and Evolution of Mammalian Ears and Hearing Function. *In*: B. Fritzsch and B. Grothe (eds.), *The Senses—A Comprehensive Reference, Volume 2, Second Edition*, 207–252. Elsevier Academic Press.

Luo, Z.-X., and Martin, T. 2007. Analysis of molar structure and phylogeny of docodontan genera. *Bulletin of Carnegie Museum of Natural History* 39: 27–47.

Luo, Z.-X. and Wu, X.-C. 1994. The small tetrapods of the lower Lufeng Formation, Yunnan, China. *In*: N.C. Fraser and H.-D. Sues (eds.), *In the Shadow of the Dinosaurs—Early Mesozoic Tetrapods*, 251–270. Cambridge University Press, Cambridge.

Luo, Z.-X., Crompton, A.W., and Sun, A.-L. 2001. A new mammaliaform from the Early Jurassic of China and evolution of mammalian characteristics. *Science* 292: 1535–1540.

Luo, Z.-X., Gatesy, S.M., Jenkins, F.A., Amaral, A.A., and Shubin, N.H. 2015a. Mandibular and dental characteristics of Late Triassic mammaliaform *Haramiyavia* and their ramifications for basal mammal evolution. *Proceedings of National Academy of Sciences USA* 112 (51): E7101–E7109.

Luo, Z.-X., Kielan-Jaworowska, Z., and Cifelli, R.L. 2002. In quest for a phylogeny of Mesozoic mammals. *Acta Palaeontologica Polonica* 47: 1–78.

Luo, Z.-X., Kielan-Jaworowska, Z., and Cifelli, R.L. 2004. Evolution of dental replacement in mammals. *Bulletin of Carnegie Museum of Natural History* 36: 159–175.

Luo, Z.-X., Lucas, S.G., Li, J.-J., and Zhen, S.-N. 1995. A new specimen of *Morganucodon oehleri* from the Lower Lufeng Formation, Yunnan, China. *Neues Jahrbuch für Geologie und Paläontologie* 11: 671–680.

Luo, Z.-X., Meng, Q.-J., Grossnickle, D.M., Liu, D., Zhang, Y.-G., Neander, A.I., and Q, Ji. 2017. New evidence for mammaliaform ear evolution and feeding adaptation in a Jurassic ecosystem. *Nature* 548: 326–329.

Luo, Z.-X., Meng, Q.-J., Ji, Q., Liu, D., Zhang, Y.-G., and Neander, A.I. 2015b. Evolutionary development in basal mammaliaforms as revealed by a docodontan. *Science* 347: 760–764.

Luo, Z.-X., Schultz, J.A., and Ekdale, E.G. 2016. Evolution of the middle and inner ears of mammaliaforms: the approach to mammals. *In*: J.A. Clack, R.R. Fay and A.N. Popper (eds.), Evolution of the Vertebrate Ear: A Paleontological Perspective. *Springer Handbooks for Auditory Research* 59: 139–174.

Macrini, T.E. 2006. *The evolution of endocranial space in mammals and non-mammalian cynodonts.* 287 pp. Ph.D. Dissertation, University of Texas, Austin.

Marsh, O.C. 1880. Notice on Jurassic mammals representing two new orders. *American Journal of Science* 20: 235–239.

Meng, Q.-J., Ji, Q., Zhang, Y.-G., Liu, D., Grossnickle, D.M., and Luo, Z.-X. 2015. An arboreal docodont from the Jurassic and mammaliaform ecological diversification. *Science* 347: 764–768.

Mills, J.R.E. 1971. The dentition of *Morganucodon. In*: D.M. Kermack and K.A. Kermack (eds.), Early Mammals. *Zoological Journal of the Linnean Society* 50 (Supplement 1): 29–63.

Mills, J.R.E. 1984. The molar dentition of a Welsh pantothere. *Zoological Journal of Linnean Society* 84: 189–205.

O'Meara, R.N. and Thompson, R.S. 2014. Were there Miocene meridolestidans? Assessing the phylogenetic placement of *Necrolestes paragonensis* and the presence of a 40 million year meridiolestidan ghost lineage. *Journal of Mammalian Evolution* 21: 271–284.

Panciroli, E.L., Benson, R.B.J., and Luo, Z.-X. 2019. The mandible and dentition of *Borealestes serendipitus* (Docodonta) from the Middle Jurassic of Skye, Scotland. *Journal of Vertebrate Paleontology* 39: e1621884.

Panciroli, E.L., Benson, R.B.J., Fernandez, V., Butler, R.J., Fraser, N.C., Luo, Z.-X., and Walsh, S. 2021. New species of mammaliaform and the cranium of *Borealestes* (Mammaliformes: Docodonta) from the Middle Jurassic of the British Isles. *Zoological Journal of Linnean Society* 192: 1323–1362.

Parrington, F.R. 1971. On the Upper Triassic mammals. *Philosophical Transactions of the Royal Society B* 261: 231–272.

Parrington, F.R. 1973. The dentitions of the earliest mammals. *Zoological Journal of the Linnean Society* 52: 85–95.

Patterson, B. and Olson, E.C. 1961. A triconodontid mammal from the Triassic of Yunnan. *In*: G. Vandebroek (ed.), *International Colloquium on the Evolution of Lower and Non-specialized Mammals*, 129–191. Koninklijke Vlaamse Academie voor Wetenschappen, Letteren en Schone Kunsten van Belgie, Brussels.

Rich, T.H., Vickers-Rich, P., Constantine, A., Flannery, T.F., Kool, L., and Van Klaveren, N. 1999. Early Cretaceous mammals from Flat Rocks, Victoria, Australia. *Records of the Queen Victoria Museum and Art Gallery* 106: 1–34.

Rigney, H.W. 1963. A specimen of *Morganucodon* from Yunnan. *Nature* 197: 1122–1123.

Rougier, G.W., Sheth, A.S., Carpenter, K., Appella-Guiscafre, L., and Davis, B.M. 2015. A new species of *Docodon* (Mammaliaformes: Docodonta) from the Upper Jurassic Morrison Formation and a reassessment of selected craniodental characters in basal mammaliaforms. *Journal of Mammalian Evolution* 22: 1–16.

Rowe, T.B. 1988. Definition, diagnosis, and origin of Mammalia. *Journal of Vertebrate Paleontology* 8: 241–264.

Rowe, T.B. 2020. The emergence of mammals. *In*: J. Kass (ed.), *Evolutionary Neuroscience, Edition 2*, 263–319, Elsevier Academic Press.

Rowe, T.B. and Shepherd, G.M. 2016. Role of ortho-retronasal olfaction in mammalian cortical evolution. *The Journal of Comparative Neurology* 524: 471–495.

Rowe, T.B., Macrini, T.E., and Luo, Z.-X. 2011. Fossil evidence on origin of the mammalian brain. *Science* 332: 955–957.

Rowe, T.B., Rich, T.H., Vickers-Rich, P., Springer, M., and Woodburne, M.O. 2008. The oldest platypus and its bearing on divergence timing of the platypus and echidna clades. *Proceedings of the National Academy of Sciences USA* 105: 1238–1242.

Ruf, I., Luo, Z.-X., and Martin, T. 2013. Re-investigation of the basicranium of *Haldanodon exspectatus* (Docodonta, Mammaliaformes). *Journal of Vertebrate Paleontology* 33: 382–400.

Schultz, J.A., Bhullar, B.A.S., and Luo, Z.-X. 2019. Re-examination of the Jurassic mammaliaform *Docodon victor* by computed tomography and occlusal functional analysis. *Journal of Mammalian Evolution* 26: 9–38.

Scott, J.E., Hogue, A.S., and Ravosa, M.J. 2012. The adaptive significance of mandibular symphyseal fusion in mammals. *Journal of Evolutionary Biology* 25: 661–673.

Sigogneau-Russell, D. and Hahn, G. 1994. Late Triassic microvertebrates from Central Europe. *In*: N.C. Fraser and H.-D. Sues (eds.), *In the Shadow of the Dinosaurs—Early Mesozoic Tetrapods*, 197–213. Cambridge University Press, Cambridge.

Smith, B.H. 2000. 'Schultz's rule' and the evolution of tooth emergence and replacement patterns in primates and ungulates. *In*: M.F. Teaford, M.M. Smith, and M.W.J. Ferguson (eds.), *Development, Function and Evolution of Teeth*, 212–227. Cambridge University Press, Cambridge.

Sulej, T., Krzesiński, G., Tałanda, M., Wolniewicz, A.S., Błażejowski, B., Bonde, N., Gutowski, P., Sienkiewicz, M., and Niedźwiedzki, G. 2020. The earliest-known mammaliaform fossil from Greenland sheds light on origin of mammals. *Proceedings of the National Academy of Sciences USA* 117: 26861–26867.

Tarver, J.E., dos Reis, M., Mirarab, S., Moran, R.J., Sean Parker, S., O'Reilly, J.E., King, B.L., O'Connell, M.J., Asher, R.J., Warnow, T., Peterson, K.J., Donoghue, P.C.J., and Pisani, D. 2016. The interrelationships of placental mammals and the limits of phylogenetic inference. *Genome Biology and Evolution* 8: 330–344.

Turnbull, W.D. 1970. Mammalian masticatory apparatus. *Fieldiana Geology* 18: 147–356.

van Nievelt, A.F.H. and Smith, K.K. 2005a. The significance of reduced functional tooth replacement in marsupial and placental mammals. *Paleobiology* 31: 324–346.

van Nievelt, A.F.H. and Smith, K.K. 2005b. Tooth eruption in *Monodelphis domestica* and its significance for phylogeny and natural history. *Journal of Mammalogy* 86: 333–341.

Waldman, M., and Savage, R.J.G. 1972. The first Jurassic mammal from Scotland. *Journal of the Geological Society of London* 128:119–125.

Ziegler, A.C. 1971. A theory of the evolution of therian dental formulas and replacement patterns. *The Quarterly Review of Biology* 46: 226–249.

Ziegler, A.C. 1972. Milk dentition in the broad-footed mole, *Scapanus latimanus*. *Journal of Mammalogy* 53: 354–345.

Zhang, F.-K., Crompton, A.W., Luo, Z.-X., and Schaff, C.R. 1998. Pattern of dental replacement of *Sinoconodon* and its implications for evolution of mammals. *Vertebrata PalAsiatica* 36: 197–217.

Zhou, C.-F., Bhullar, B.-A.S., Neander, A.I., Martin, T., and Luo, Z.-X. 2019. New Jurassic mammaliaform sheds light on early evolution of mammal-like hyoid bones. *Science* 365: 276–279.